



1 **Identifying decadal trends in deweathered concentrations of criteria air pollutants**  
2 **in Canadian urban atmospheres with machine learning approaches**

3

4 Xiaohong Yao<sup>1,\*</sup>, Leiming Zhang<sup>2,\*</sup>

5 <sup>1</sup> Key Laboratory of Marine Environment and Ecology (MoE), Frontiers Science Center  
6 for Deep Ocean Multispheres and Earth System, and Sanya Oceanographic Institution,  
7 Ocean University of China, Qingdao 266100, China

8 <sup>2</sup> Air Quality Research Division, Science and Technology Branch, Environment and  
9 Climate Change Canada, 4905 Dufferin Street, Toronto, Ontario, M3H 5T4, Canada

10 \*Corresponds to: [xhyao@ouc.edu.cn](mailto:xhyao@ouc.edu.cn), [leiming.zhang@ec.gc.ca](mailto:leiming.zhang@ec.gc.ca)

11

12 **Abstract.** This study investigates long-term trends of criteria air pollutants, including  
13 NO<sub>2</sub>, CO, SO<sub>2</sub>, O<sub>3</sub> and PM<sub>2.5</sub>, and (NO<sub>2</sub>+O<sub>3</sub>) measured in ten Canadian cities during the  
14 last two to three decades and associated driving forces in terms of emission reductions,  
15 perturbations from varying weather conditions and large-scale wildfires, and changes  
16 in O<sub>3</sub> sources and sinks. Two machine-learning methods, including random forest  
17 algorithm and boosted regression trees, were used to extract deweathered mixing ratios  
18 (or mass concentrations) of the pollutants. The Mann-Kendall analysis of the  
19 deweathered and original annual average concentrations of the pollutants showed that,  
20 on the time scale of 20 years or longer, the perturbation from varying weather  
21 conditions exerted a very minor influence on the decadal trends of original annual  
22 averages (within ±2%) in ~70% of the cases, and a moderate influence up to 16% of  
23 the original trends in the other 30% cases. NO<sub>2</sub>, CO and SO<sub>2</sub> showed decreasing trends  
24 in the last two to three decades in all the cities except CO in Montreal. O<sub>3</sub> showed  
25 increasing trends in all the cities, except Halifax, mainly due to weakened titration  
26 reaction between O<sub>3</sub> and NO. (NO<sub>2</sub>+O<sub>3</sub>), however, showed decreasing trends in all the  
27 cities, except Victoria, because the increase in O<sub>3</sub> is much less than the decrease in NO<sub>2</sub>.  
28 In three of the five eastern Canadian cities, emission reductions dominated the



29 decreasing trends in  $PM_{2.5}$ , but no significant trends in  $PM_{2.5}$  were observed in the other  
30 two cities. In five western Canadian cities, increasing or no significant trends in  $PM_{2.5}$   
31 were observed, likely due to unpredictable large-scale wildfires overwhelming or  
32 balancing the impacts of emission reductions on  $PM_{2.5}$ . In addition, despite improving  
33 air quality during the last two decades in most cities, air quality health index of above  
34 10 (representing very high-risk condition) still occasionally occurred after 2010 in  
35 western Canadian cities because of the increased large-scale wildfires.

36

37 **Keywords:** Atmospheric pollutants, trend analysis, machine learning, emission  
38 reduction, wildfire emission

## 39 **1 Introduction**

40 Criteria air pollutants can harm human health and the natural environment. According  
41 to Health Impacts of Air pollution in Canada 2021 Report (Health Canada, 2021), it is  
42 estimated that air pollution of  $NO_2$ ,  $O_3$  and  $PM_{2.5}$  caused 15,300 deaths per year,  
43 corresponding to 42 deaths per 100,000 population in Canada in 2016. To protect  
44 human health and the Environment, the Canadian Council of Ministers of the  
45 Environment (CCME) developed the Canadian Ambient Air Quality Standards  
46 (CAAQS) for  $PM_{2.5}$ ,  $O_3$ ,  $SO_2$  and  $NO_2$ . CAAQS are supported by four colour-coded  
47 management levels with each management level being determined by the amount of a  
48 pollutant within an air zone, from which recommendations on air quality management  
49 actions are provided. Following this standard, multiphase mitigation measures have  
50 been implemented to largely reduce anthropogenic air pollutant emissions in recent  
51 decades (ECCC, 2021). Air quality in Canadian urban atmospheres well meets CAAQS  
52 in recent years, as reported in Air Quality- Canadian Environmental Sustainability  
53 Indicators (ECCC, 2023).

54

55 Nevertheless, the World Health Organization (WHO, 2021) updated the global air  
56 quality guidelines (AQG) on  $NO_2$ ,  $SO_2$ ,  $CO$ ,  $O_3$  and  $PM_{2.5}$  in 2021, based on



57 accumulated strong evidence that air pollution can affect public health even at very low  
58 concentrations. In the WHO 2021 AQG, NO<sub>2</sub> annual average concentration is set as 10  
59 µg m<sup>-3</sup>, equivalent to ~ 5 ppb at annual average temperatures of 6-10 °C across Canada,  
60 annual average and 24-hour average PM<sub>2.5</sub> concentrations are set as 5 µg m<sup>-3</sup> and 15 µg  
61 m<sup>-3</sup>, respectively, and peak season mean 8-hr ozone concentration is set as 60 µg/m<sup>3</sup>.  
62 Recent studies showed that over 95% cities worldwide face more challenges to further  
63 lower ambient NO<sub>2</sub>, O<sub>3</sub> and PM<sub>2.5</sub> concentrations in order to meet the WHO 2021 AQG  
64 (Dabek-Zlotorzynska et al., 2019; Griffin et al., 2020; Xu et al., 2019; Jeong et al., 2020;  
65 Al-Abadleh et al., 2021; Wang et al., 2021; Zhang et al., 2022; Bowdalo et al., 2022).

66  
67 In search for the most efficient mitigation measures for criteria pollutants, the  
68 effectiveness of existing measures on air pollution reduction needs to be first examined.  
69 For this purpose, long-term trends in concentrations of the criteria air pollutants need  
70 to be quantified and the driving forces of the trends, besides anthropogenic emission  
71 reductions, should be identified. Several studies have investigated the decadal trends of  
72 criteria pollutants in Canada in the past decade. For example, Chan and Vet (2010)  
73 reported upward trends in O<sub>3</sub> mixing ratio from 1997-2006 at dozens of sites in Canada.  
74 Xu et al. (2019) and Zhang et al. (2022) also found increasing trends in O<sub>3</sub> mixing ratio  
75 from 1996-2016 at multiple sites in Windsor, Ontario, which was attributed to the  
76 reduced titration effect of NO with O<sub>3</sub>. They also reported that the 95<sup>th</sup> percentile O<sub>3</sub>  
77 mixing ratio exhibited a decreasing trend and attributed the decrease to anthropogenic  
78 emission reductions. Mitchell et al. (2021) reported that the 99<sup>th</sup> percentile O<sub>3</sub> mixing  
79 ratios exhibited a decreasing trend from 2000-2018 at urban and regional sites in Nova  
80 Scotia, but such a trend was not found for low-moderate percentile O<sub>3</sub> mixing ratios.  
81 Bari and Kindzierski (2016) found no significant trends in PM<sub>2.5</sub> mass concentration,  
82 although decreasing trends in organic carbon and element carbon from 2007-2014 in  
83 Edmonton. Jeong et al. (2020) reported 34% decrease in PM<sub>2.5</sub> mass concentration from  
84 2004-2017 in Toronto and attributed the decrease to the reduced coal-fired power plants  
85 emissions. Wang et al. (2022a) reported significant decreasing trends in organic and



86 elemental carbon in PM<sub>2.5</sub> from 2003-2019 at seven urban sites in Canada. Studies on  
87 other criteria pollutants are very limited (Feng et al., 2020; Jeong et al.; 2020).

88  
89 O<sub>3</sub> mixing ratios, especially at high levels, are strongly affected by meteorological  
90 conditions, and thus, ozone trends on the decadal scale can be perturbed by varying  
91 weather conditions from year to year (Simon et al., 2015; Xing et al., 2015; Ma et al.,  
92 2021; Lin et al., 2022). Inter-annual variations of weather conditions also have strong  
93 impact on the decadal trends of other criteria pollutants (Lin et al., 2022). Air quality  
94 models are useful tools to analyze emission-driven air quality trends and meteorological  
95 impacts (Foley et al., 2015; Astitha et al., 2017; Vu et al., 2019), but most modeling  
96 results suffer from large uncertainties, which could exceed annual average changes of  
97 the simulated pollutants. The machine learning techniques have been demonstrated to  
98 be a powerful tool to decouple impacts of emission changes and perturbations from  
99 varying weather and/or meteorological conditions, enabling the derivation of  
100 deweathered trends in air pollutants concentrations (Grange and Carslaw, 2019; Ma et  
101 al., 2021; Mallet, 2021; Shi and Brasseur, 2020; Wang et al., 2020; Munir et al., 2021;  
102 Lovric et al., 2021; Hou et al., 2022; Lin et al., 2022).

103  
104 This study attempts to deduct the perturbations from varying weather conditions on the  
105 observed mixing ratios (or mass concentrations) of criteria air pollutants in Canada  
106 during the past two to three decades and thereby investigates their emission-driven  
107 trends. We used two machine-learning methods, including the random forest (RF)  
108 algorithm and boosted regression trees (BRTs), to generate the deweathered mixing  
109 ratios (or concentrations) of NO<sub>2</sub>, SO<sub>2</sub>, CO, O<sub>3</sub>, (NO<sub>2</sub>+O<sub>3</sub>) and PM<sub>2.5</sub> during the past  
110 decades in ten cities equally distributed in eastern and western Canada. Considering  
111 that the machine-learning methods may suffer from the weakness in accurately  
112 predicting large percentile concentrations of criteria air pollutants, we also applied our  
113 previously developed identical-percentile autocorrelation analysis method to accurately  
114 quantify the perturbations from extreme events such as large-scale wildfires on large



115 percentile PM<sub>2.5</sub> concentrations (Yao and Zhang, 2020; Lin et al., 2022). The Mann-  
116 Kendall (M-K) analysis was then employed to resolve the trends in the deweathered  
117 mixing ratios (or mass concentrations). To establish the relationship between air  
118 pollutants concentrations and emission reductions, the deweathered and original mixing  
119 ratios (or mass concentrations) of the air pollutants were correlated with the  
120 corresponding provincial-level emissions. In addition, the Air Quality Health Index  
121 (AQHI, [https://weather.gc.ca/airquality/pages/index\\_e.html](https://weather.gc.ca/airquality/pages/index_e.html)), a health protection tool  
122 designed in Canada to advise the public to adjust outdoor activities based on air  
123 pollution levels, were also analyzed with particular attention to the trends with AQHI  
124 being above 7 and 10. This study provides a thorough assessment of the emission-  
125 driven trends in criteria pollutants on the time scale of two to three decades across  
126 Canadian urban atmospheres, knowledge from which is much needed in developing  
127 future emission control policies of the concerned pollutants.

## 128 **2 Methodology**

### 129 **2.1 Monitoring sites and data sources**

130 Ten major cities, including five in eastern Canada (Halifax, Quebec, Montreal, Toronto  
131 and Hamilton) and five in western Canada (Winnipeg, Calgary, Edmonton, Vancouver  
132 and Victoria), from the National Air Pollution Surveillance (NAPS) program are  
133 selected for investigating decadal trends of the monitored criteria pollutants (Table S1).  
134 The NAPS program has long-term air quality data of a uniform standard across Canada  
135 (Dabek-Zlotorzynska et al., 2011, 2019; Jeong et al., 2020; Yao and Zhang, 2020; Wang  
136 et al., 2021, 2022a). The NAPS program includes both continuous and time-integrated  
137 measurements of gaseous and particulate air pollutants. Continuous data are available  
138 as hourly concentrations and are quality-assured as specified in the Ambient Air  
139 Monitoring and Quality Assurance/Quality Control Guidelines  
140 (<https://open.canada.ca/data/en/dataset/1b36a356-defd-4813-acea-47bc3abd859b>).

141

142 Multiple monitoring sites exist in most cities. In each city selected above, data at only



143 one site with the most complete dataset of the five criteria pollutants (NO<sub>2</sub>, CO, SO<sub>2</sub>,  
144 O<sub>3</sub> and PM<sub>2.5</sub>) and the longest data record were selected for analysis in this study (Table  
145 S1). In cases with a data gap longer than a year, data at a nearby site (within 1 km) were  
146 then used to fill the gap. If no site within 1 km is available, then the data gap is left  
147 unfilled. SO<sub>2</sub>, CO, NO<sub>x</sub> and PM<sub>2.5</sub> emission data at the provincial level in Canada are  
148 obtained from [https://www.canada.ca/en/environment-climate-](https://www.canada.ca/en/environment-climate-change/services/environmental-indicators/air-pollutant-emissions.html)  
149 [change/services/environmental-indicators/air-pollutant-emissions.html](https://www.canada.ca/en/environment-climate-change/services/environmental-indicators/air-pollutant-emissions.html).

150 Besides the monitored criteria pollutants described above, AQHI is also calculated in  
151 this study at three-hour resolution using the following formula (Stieb et al., 2008; To et  
152 al., 2013):

153  $AQHI = (100/10.4) * [(e^{0.000537*O_3-1}) + (e^{0.000871*NO_2-1}) + (e^{0.000537*PM_{2.5}-1})]$ , in which  
154 O<sub>3</sub> and NO<sub>2</sub> represent their respective three-hour average original mixing ratios (in ppb)  
155 and PM<sub>2.5</sub> represents its three-hour average original concentration (in µg m<sup>-3</sup>). The  
156 calculated AQHI is rounded to the nearest positive integer. AQHI between 1-3  
157 represents excellent air quality that is safe for outdoor activities. Outdoor activities may  
158 be reduced at AQHI between 4-6 for certain population with some health issues. AQHI  
159 between 7-10 and >10 correspond to high and very high health risk conditions,  
160 respectively. Note that four alternative AQHI-Plus amendments have been proposed for  
161 wildfire seasons and the AQHI-Plus values are always larger than the corresponding  
162 AQHI values (Yao et al., 2020). One of AQHI-Plus amendments has been implemented  
163 in late 2016 in British Columbia Province. The AQHI-Plus amendments are not used in  
164 this study since it is not implemented across the whole Canada.

165

## 166 **2.2 Statistical analysis**

167 In this study, two popular machine-learning packages, including the “rmweather” R  
168 package (Grange et al., 2018) and the “deweather” R package (Carslaw and Ropkins,  
169 2012; Carslaw and Taylor, 2009), were used to perform the RF algorithm and the BRTs,  
170 respectively. Besides the monitored hourly average mixing ratio (or mass concentration)  
171 of a pollutant, temporal variables (hour, day, weekday, week and month) and



172 meteorological parameters (wind speed, wind direction, air temperature, relative  
173 humidity and dew point) are also needed as additional independent inputs to the  
174 machining learning process. The hourly meteorological data were obtained from the  
175 meteorological observational station at a nearby airport in each city, which are  
176 accessible from the NOAA Integrated Surface Database (ISD) by using the “worldmet”  
177 R package (Carslaw, 2021). The meteorological data from the nearest airport in every  
178 city should reflect synoptic weather conditions, which have been used in existing  
179 machine learning studies (Vu et al., 2019; Mallet, 2020; Wang et al., 2020; Dai et al.,  
180 2021; Ma et al., 2021). Additional meteorological parameters such as boundary layer  
181 height, total cloud cover, surface net solar radiation, surface pressure, total precipitation  
182 and air mass clusters have also been used in some studies to improve the performance  
183 of the machine learning methods (Hou et al., 2022; Shi et al., 2021; Lin et al., 2022).  
184 These additional meteorological parameters were not included in the present study  
185 because they are not available in earlier years of the study period. Nevertheless, good  
186 performance can still be achieved in the present study mainly because of multi-decade  
187 length of the datasets, as demonstrated by an example shown in Fig. 1. Note that the  
188 inputs for the two packages were randomly divided into two groups, i.e., the training  
189 dataset that used 80% of the data and a testing dataset that used the remaining 20%. The  
190 testing datasets were different between the RF algorithm and the BRTs.

191  
192 Five statistical metrics, including determination coefficient ( $R^2$ ), root mean square error  
193 (RMSE), mean bias (MB), mean fractional bias (MFB) and mean fractional error  
194 (MFE), were calculated to evaluate the performance of the two machine-learning  
195 methods. In the literature, criteria and goal values have not been set for the statistical  
196 metrics for the purpose of evaluating machine-learning prediction performance.  
197 Alternatively, the criteria and goal values for MFE and MFB proposed by USEPA are  
198 adopted here, which are  $MFE \leq 75\%$  and  $MFB \leq \pm 60\%$  for the criteria value and  $MFE \leq 50\%$   
199 and  $MFB \leq \pm 30\%$  for the goal value (USEPA, 2007).

200



201 Fig. 1 shows predictions against observations of NO<sub>2</sub> mixing ratio in Halifax during  
202 1996-2017, as an example for evaluating the performance of the two machining  
203 methods. MFB and MFE values were far below their respective goal values for both  
204 RF algorithm and BRTs set by USEPA. R<sup>2</sup> and RMSE were 0.86 and 5.1, respectively,  
205 for both methods. MB is -0.04 for RF algorithm and 0.1 for BRTs. The values of these  
206 metrics indicated that the predictions reasonably well reproduced the observations.  
207 However, the two machine learning methods overall underpredicted NO<sub>2</sub> mixing ratios  
208 to a small extent based on the regression lines slightly below the 1:1 line. The  
209 underestimation was mainly due to sporadic large values in the measurement of NO<sub>2</sub>  
210 mixing ratio, which did not provide sufficient samples for the machine-learning  
211 methods to learn and yield good prediction. For all the pollutants in all the cities  
212 investigated in this study, the machine-learning predictions generally met the goal  
213 values set by USEPA, except for PM<sub>2.5</sub> in some western Canadian cities such as Calgary  
214 and Edmonton with the predictions only meeting criteria values because of the  
215 perturbation from large-scale wildfires.

216

217 Following the approach described in earlier studies (Hou et al., 2022; Lin et al., 2022),  
218 the two machine learning methods were run for 1000 times with meteorological  
219 variables randomly resampled from the study period. The average model prediction  
220 from the 1000 model runs represents the meteorologically normalized pollutant  
221 concentration at a particular time. We also tested averaging 2000 and 3000 model  
222 predictions, which produced consistent results with those of using 1000 model  
223 predictions. Thus, averaging 1000 model predictions was used for meteorological  
224 normalization in this study.

225

226 As mentioned above, the machine learning methods suffer from the weakness in  
227 accurately predicting high concentration values. We thus applied the identical-  
228 percentile autocorrelation analysis method developed in our previous study to quantify  
229 the perturbations from extreme events such as large-scale wildfires on the large





230 percentile concentration values (Yao and Zhang, 2020; Lin et al., 2022). The method  
231 has five steps for data processing and analysis. The first step is to construct a long-term  
232 average data series at hourly resolution covering 365 days by averaging the  
233 corresponding hourly data from all the years of the study period. The second step is to  
234 pair a data series at any given year to the long-term average data series, and if there  
235 were any data gaps (missing hours) in the former data series, data for these hours in the  
236 latter series were also removed so that the two data series have exactly the same size.  
237 The third step is to rearrange all the hourly data from the smallest to the largest value  
238 in each of the data series generated in step 2, and then conduct correlation analysis  
239 between the pair of data series. Inflection points in the large and small percentile zone  
240 were first visibly identified/guessed, and referenced as upper and lower inflection  
241 points, respectively. The pair of data between the lower and upper inflection points were  
242 correlated repeatedly by varying values of the two inflection points in search for highest  
243  $R^2$  values. The fourth step is to predict the large percentile values exceeding the upper  
244 inflection point using the regression equation with the highest  $R^2$  generated in step 3.  
245 The final step is to obtain the perturbations from extreme events on the large percentile  
246 concentrations by subtracting the observed values from the predicted values.  
247 Fig. 2 shows three examples calculating the perturbations from varying weather  
248 conditions and large-scale wildfires on the large percentile concentrations of  $PM_{2.5}$  in  
249 1998, 1999 and 2019 in Edmonton. Large-scale wildfires occurred in 1998 and 2019  
250 (Fig. S1), but no record in 1999. In 1998, data points outside the 4.5<sup>th</sup>-94<sup>th</sup> percentile  
251 range were screened out through steps 1-3, and the remaining data points were used to  
252 obtain a regression equation, which shows  $[PM_{2.5}]_{data\ in\ 1998} = [PM_{2.5}]_{long-term\ average} * 3.9-$   
253  $18$  ( $R^2=0.96$ ,  $P<0.01$ ) (Fig. 2a).  $[PM_{2.5}]_{data\ in\ 1998}$  and  $[PM_{2.5}]_{long-term\ average}$  represent the  
254 same identical percentile values of  $PM_{2.5}$  in re-organized data series of 1998 and the  
255 long-term average through steps 1-3, respectively. The similar definition is applicable  
256 for  $[PM_{2.5}]_{data\ in\ 1999}$  and  $[PM_{2.5}]_{data\ in\ 2019}$  presented below. In 1999, data points within  
257 the 4.5<sup>th</sup>-99.7<sup>th</sup> percentile range resulted in a regression equation of  $[PM_{2.5}]_{data\ in\ 1999} =$   
258  $[PM_{2.5}]_{long-term\ average} * 3.1-15$  ( $R^2=0.97$ ,  $P<0.01$ ) (Fig. 2c). In 2019, data points within



259 the 5.4<sup>th</sup>–96<sup>th</sup> percentile range resulted in  $[PM_{2.5}]_{data\ in\ 2019} = [PM_{2.5}]_{long-term\ average} * 2.2-$   
260  $12 (R^2=0.94, P<0.01)$  (Fig. 2e). Note that step 3 is critical to obtain these excellent good  
261 correlations (Fig. 2a, c and e) as compared with those absent of step 3 (Fig. 2b, d and  
262 f).

263

264 The perturbation from the extreme weather conditions or the extreme events on the  
265 100<sup>th</sup> percentile  $PM_{2.5}$  value at a particular year ( $y$ ) can be calculated as:

$$266 [PM_{2.5}]_{perturbation\ at\ 100th,y} = [PM_{2.5}]_{predicted\ at\ 100th,y} - [PM_{2.5}]_{observed\ at\ 100th,y}$$

$$267 [PM_{2.5}]_{predicted\ at\ 100th,y} = [PM_{2.5}]_{long-term\ average\ at\ 100th} * k_y + b_y$$

268 where  $[PM_{2.5}]_{observed\ at\ 100th,y}$  represents the 100<sup>th</sup> percentile  $PM_{2.5}$  value observed in  $y$   
269 year;  $k_y$  and  $b_y$  represent the slope and intercept, respectively, of the regression equation  
270 with the highest  $R^2$  in the  $y$  year generated through steps 1-3. Similarly, the perturbation  
271 inherent from the large percentile values from the final upper infection point ( $m^{th}$ ) to  
272 100<sup>th</sup> percentile in a particular year can be calculated as:

$$273 [PM_{2.5}]_{perturbation\ at\ \geq mth,y} = [PM_{2.5}]_{predicted\ at\ \geq mth,y} - [PM_{2.5}]_{observed\ at\ \geq mth,y},$$

$$274 [PM_{2.5}]_{predicted\ at\ mth,y} = [PM_{2.5}]_{long-term\ average\ at\ mth} * k_y + b_y$$

275 The calculated values from  $[PM_{2.5}]_{perturbation\ at\ \geq mth,y}$  to  $[PM_{2.5}]_{perturbation\ at\ 100th,y}$  in the  $y$   
276 year were averaged as  $[PM_{2.5}]_{perturbation\ average,y}$ . The perturbation contribution to the  
277 corresponding original annual average equals to  $[PM_{2.5}]_{perturbation\ average,y} * (1-m\%)$  in  $y$   
278 year, and the values were  $3.0\ \mu g\ m^{-3}$  in 1998,  $0.2\ \mu g\ m^{-3}$  in 1999 and  $1.7\ \mu g\ m^{-3}$  in 2019  
279 in Edmonton, corresponding to strong, negligible and moderate perturbations,  
280 respectively, from large wildfires.

281

282 The M-K analysis is employed to resolve the trends in the time series of the  
283 deweathered and original annual average concentration of each pollutant. Qualitative  
284 trends revolved by the M-K method include 1) an increasing or decreasing trend with a  
285 P value of  $<0.05$ , and 2) no significant trend including a probably increasing or  
286 decreasing trend, a stable trend, and a no-trend with all the other conditions (Aziz et al.,  
287 2003; Kampata et al., 2008; Yao and Zhang, 2020). The extracted trends and associated



288 driving factors are discussed in detail below.

289

### 290 **3. Results**

#### 291 *3.1 Trends in deweathered and original NO<sub>2</sub> mixing ratios*

292 Fig. 3a and b show decadal variations in the original annual averages of NO<sub>2</sub> mixing  
293 ratios in the ten Canadian cities. The BRTs-deweathered and RF-deweathered hourly  
294 averages of NO<sub>2</sub> mixing ratios are shown in Fig S2, in which the deweathered results  
295 were also interpreted in terms of increased or reduced emissions of NO<sub>x</sub>. The decadal  
296 trends resulted from annual averages of BRTs-deweathered, RF-deweathered and  
297 original NO<sub>2</sub> mixing ratios are listed in Table 1.

298

299 The deweathered and original annual average NO<sub>2</sub> mixing ratios in any of the 10 cities  
300 both showed consistent decreasing trends in the last 2-3 decades ( $P < 0.05$  through M-K  
301 analysis). The BRTs-deweathered and RF-deweathered annual averages highly  
302 correlated with the original values with  $R^2 > 0.95$  and  $P < 0.01$  (Table 1). The slopes of  
303 zero-intercept regression equations between the deweathered and original annual  
304 average NO<sub>2</sub> mixing ratios were mostly within 0.98-1.04, indicating  $\leq 4\%$  differences  
305 between the deweathered and original annual values. These results indicated that the  
306 perturbation from varying weather conditions only exerted minor influences on the  
307 original annual averages. The only exception is the RF-deweathered annual averages in  
308 Halifax (with a slope of 1.08); however, this may not suggest that the perturbation from  
309 varying weather conditions was as high as 8% since the BRTs-deweathered annual  
310 averages in the same city showed a slope of only 1.03, indicating that the methodology  
311 uncertainties can be as large as 5%.

312

313 The annual decreasing rates in the deweathered and original NO<sub>2</sub> mixing ratios in the  
314 studied cities varied from 0.31 to 0.74 ppb year<sup>-1</sup>, and the overall percentage decreases  
315 ranged from 37% to 62% during the last two to three decades (Table 1). Our results  
316 suggested that varying weather conditions likely played a negligible role in the annual



317 decreasing rates of NO<sub>2</sub> mixing ratio in two eastern (Montreal and Hamilton) and four  
318 western (Winnipeg, Calgary, Vancouver and Victoria) Canadian cities, as can be seen  
319 from the very close annual decreasing rates between the deweathered and original  
320 annual average mixing ratios, despite methodology uncertainties in generating  
321 deweathered mixing ratios as mentioned above. In the remaining four cities, the annual  
322 decreasing rates were always larger in the original than the deweathered annual average  
323 NO<sub>2</sub> mixing ratio, with the largest differences in Toronto (0.07-0.10 ppb year<sup>-1</sup>),  
324 followed by Halifax (0.06-0.10 ppb year<sup>-1</sup>), Edmonton (0.06-0.08 ppb year<sup>-1</sup>) and  
325 Quebec (0.02-0.07 ppb year<sup>-1</sup>), suggesting that varying weather conditions contributed  
326 appreciably to the annual decreasing rate. The annual decreasing rates were highly city-  
327 dependent, but there were no significant differences between eastern and western cities  
328 ( $P>0.05$ ). With continuously decreasing NO<sub>2</sub> mixing ratios in the last decades (Fig. 3),  
329 annual average NO<sub>2</sub> fell to below 10 ppb by 2019 in half of the studied cities (Halifax,  
330 Montreal, Quebec, Winnipeg and Victoria), meeting the WHO 2021 guideline.  
331 Additional efforts are still needed to lower the NO<sub>2</sub> level in the rest of the cities,  
332 especially in Toronto and Edmonton in which annual average NO<sub>2</sub> were still as high as  
333 15 ppb in 2019.

334

335 NO<sub>2</sub> in urban atmospheres were mainly formed by the rapid titration reaction of NO  
336 with O<sub>3</sub>, with NO largely released from anthropogenic emissions, especially the  
337 transport sector (Pappin et al., 2016; Casquero-Vera et al., 2019; Dabek-Zlotorzynska  
338 et al., 2019; Feng et al., 2020; Griffin et al., 2020; Al-Abadleh et al., 2021). The  
339 correlations between the annual average NO<sub>2</sub> mixing ratios and corresponding  
340 provincial NO<sub>x</sub> emissions were thereby analyzed below (Table 1). Note that the on-line  
341 air pollutant emission inventory in Canada reports the emissions since 1990 (ECCC,  
342 2021) so the correlation analysis only covers the period of 1990-2019. Good  
343 correlations ( $R^2=0.82-0.98$ ) were obtained in all of the five eastern Canadian cities. The  
344 overall decreasing percentages of the deweathered and original NO<sub>2</sub> mixing ratios in  
345 Halifax and Quebec were roughly the same as that of the provincial grand total and



346 transportation  $\text{NO}_x$  emissions, but in Montreal, Toronto and Hamilton the former  
347 decreasing percentages were smaller than the latter ones. In contrast, the overall  
348 decreasing percentages in  $\text{NO}_2$  mixing ratio in the five western Canadian cities were  
349 substantially larger than the corresponding decreasing percentages of the provincial  
350 grand total and transportation  $\text{NO}_x$  emissions, and the correlation ( $R^2=0.54-0.94$ )  
351 between  $\text{NO}_2$  mixing ratio and provincial emission were not as good as those in eastern  
352 cities. The extreme case occurred in Calgary, where  $\text{NO}_2$  mixing ratio decreased by 31-  
353 33% during 1990-2007 when the grand total and transportation  $\text{NO}_x$  emissions in  
354 Alberta province increased by 11% and 5%, respectively, noting that a much short  
355 period of data were used in this than other cities.

356

### 357 *3.2 Trends in deweathered and original mixing ratios of CO and SO<sub>2</sub>*

358 The original annual average mixing ratios of CO and  $\text{SO}_2$  in the ten cities generally met  
359 the WHO 2021 air quality guidelines in the last decade, except  $\text{SO}_2$  in Hamilton (Fig.  
360 S4). Thus, the analysis results on deweathered and original mixing ratios of  $\text{SO}_2$  and  
361 CO in the nine cities and CO in Hamilton were only briefly summarized below, leaving  
362  $\text{SO}_2$  in Hamilton to be discussed separately.

363

364 The annual averages of the deweathered CO mixing ratios were reasonably consistent  
365 with the original annual averages in five cities, e.g., the slopes of the deweathered  
366 mixing ratios against the original ones varied from 0.97 to 1.03 in Montreal, Hamilton,  
367 Winnipeg, Edmonton, Vancouver and Victoria, although somewhat large differences  
368 between the deweathered and original mixing ratios were seen in Quebec with a slope  
369 of 1.12 (RF vs. Origin) and Toronto with a slope of 0.92 (BRTs vs. Origin). CO  
370 decreased by  $\geq 82\%$  in the last 2-3 decades in six cities, including Halifax (90-92%),  
371 Calgary (90-91%), Winnipeg (84-88%), Edmonton (86-86%), Toronto (83-86%) and  
372 Vancouver (82-83%) (Table S2), followed by 66-70% in Hamilton and less than 60%  
373 in Quebec (56-58%) and Victoria (57-59%). Large percentage decreases in baseline CO  
374 mixing ratios across North America were reported before (Zhou et al., 2017). The



375 deweathered and original annual averages of CO mixing ratio significantly correlated  
376 with the corresponding provincial grand total and transportation emissions of CO ( $R^2$   
377 =0.68-0.96,  $P<0.01$ ) in these nine cities. The overall percentage decreases in CO mixing  
378 ratio were nearly the same as those in the corresponding provincial transportation  
379 emissions of CO in Quebec and Victoria; however, the former percentage decreases  
380 were evidently larger than the latter ones in the other seven cities mentioned above. In  
381 Montreal, no significant trends were obtained in the deweathered and original CO  
382 mixing ratios during 1995-2010 ( $P>0.05$ ), despite that the provincial total and  
383 transportation CO emissions decreased by 37% and 53%, respectively, during the same  
384 period.

385

386 The deweathered and original annual average mixing ratios of  $SO_2$  decreased by 89-97%  
387 in the last 2-3 decades in four cities, including Winnipeg (95-97%), Vancouver (90-  
388 95%), Toronto (89-95%) and Halifax (90-93%), followed by 79-86% in Montreal, 78-  
389 85% in Quebec, 73-82% in Victoria, 62-64% in Calgary and 52-55% in Edmonton.  
390 Large percentage decreases in  $SO_2$  mixing ratio have been reported in rural atmospheres  
391 across North America during the last 2-3 decades (Xing et al., 2015; Feng et al., 2020).  
392 Since 1990, the overall decreasing percentages in  $SO_2$  mixing ratio in Halifax, Toronto,  
393 Calgary and Vancouver were evidently larger than those of the corresponding provincial  
394 grand total  $SO_2$  emissions. In Montreal, Quebec, Winnipeg and Edmonton, the  
395 percentage decreases in  $SO_2$  mixing ratio were close to those in the corresponding  
396 provincial grand total  $SO_2$  emissions during the same periods. Although  $SO_2$  mixing  
397 ratio in Victoria decreased by 73-82% during 1999-2019, the corresponding provincial  
398 grand total  $SO_2$  emission did not decrease much during the same period, suggesting the  
399 significant impact of regional transport on the continental scale. Note that the  
400 differences between the two deweathered mixing ratios of  $SO_2$  were enlarged to some  
401 extent in comparison with other pollutants, e.g., with the differences being 10-12% for  
402  $SO_2$ , but only 2-5% for  $NO_2$  (as presented above), in Montreal, Toronto and Winnipeg.  
403 The increased uncertainties led to the difference between the RF-deweathered and



404 original SO<sub>2</sub> mixing ratios being up to 16% in Winnipeg.

405

406 In Hamilton, the annual average of the deweathered SO<sub>2</sub> mixing ratios were highly  
407 consistent with those of the original data as indicated by the close to 1.0 slopes. The  
408 deweathered and original annual averages of SO<sub>2</sub> mixing ratios decreased by 23-28%  
409 during 1996-2019, which were substantially smaller than the 81% decrease of the  
410 corresponding provincial grand total SO<sub>2</sub> emissions during the same period. Such a big  
411 discrepancy indicates that the reduction in SO<sub>2</sub> emission in Hamilton likely  
412 substantially lagged behind the average provincial level. This also caused the weak  
413 correlations between annual average SO<sub>2</sub> mixing ratio in this city and provincial total  
414 SO<sub>2</sub> emission ( $R^2 = 0.42-0.57$ ,  $P < 0.05$ ). In addition, the original annual average SO<sub>2</sub>  
415 mixing ratio increased from 3.2-3.5 ppb in 2016-2017 to 4.8-5.0 ppb in 2018-2019  
416 when provincial total SO<sub>2</sub> emission changed little. Thus, reducing local SO<sub>2</sub> emissions  
417 in Hamilton is critical to further lower SO<sub>2</sub> mixing ratio in this city in order to meet the  
418 CAAQS and the WHO 2021 guideline, despite the existence of other factors such as  
419 regional transport (Zhou et al., 2017; Ren et al., 2020).

420

### 421 *3.3 Trends in deweathered and original O<sub>3</sub> and O<sub>3</sub>+NO<sub>2</sub> mixing ratios*

422 The original annual averages of O<sub>3</sub> and NO<sub>2</sub>+O<sub>3</sub> are shown in Fig. S5 and the analysis  
423 results of deweathered and original annual averages are listed in Table S4. Increasing  
424 trends in the deweathered and original annual average O<sub>3</sub> mixing ratio were obtained in  
425 nine cities during the last 2-3 decades, with Halifax as an only exception that showed  
426 no significant trend ( $P > 0.05$ ) during 2000-2017. Theoretically, the increasing trends in  
427 the O<sub>3</sub> mixing ratios could be caused by the enhanced tropospheric photochemical  
428 formation of O<sub>3</sub> and/or the weakened titration reaction between O<sub>3</sub> and NO due to the  
429 substantial reduction of NO emissions (Simon et al., 2015; Zhou et al., 2017; Sicard et  
430 al., 2020; Mitchell et al., 2021; Wang et al., 2022b) (more discussion in Section 4.1  
431 below). In contrast, the decreasing trends in the deweathered and original annual  
432 average NO<sub>2</sub>+O<sub>3</sub> mixing ratios were generally obtained, except in Victoria where there



433 was no significant trend ( $P > 0.05$ ) during 2000-2017. The opposite long-term trends  
434 between  $O_3$  and  $NO_2 + O_3$  suggested that the increase in  $O_3$  is much less than the decrease  
435 in  $NO_2$ , which does not support the hypothesis of the enhanced tropospheric formation  
436 of  $O_3$ .

437

438 The deweathered and original annual average  $O_3$  mixing ratios increased by 10 ppb in  
439 Edmonton from 1981-2019, 8 ppb in Hamilton from 1996-2019 and Calgary from  
440 1986-2014, and  $< 7$  ppb in the other cities (Fig. S5, Table S4). The increased  $O_3$  mixing  
441 ratio values likely reflected the lower limit resulted from the reduced titration reaction  
442 between  $O_3$  and NO (Simon et al., 2015; Xing et al., 2015). Varying weather conditions  
443 likely exerted a negligible influence on the decade increases in  $O_3$  mixing ratio in  
444 Edmonton, Hamilton, Calgary and Vancouver on the basis of the almost identical  
445 increases in deweathered and original annual averages. However, the comparison  
446 between deweathered and original annual averages also showed that varying weather  
447 conditions did cause an increase of 2 ppb out of the total of 7 ppb increase in the original  
448 annual average  $O_3$  in Winnipeg from 1985-2018, 1 ppb increase in Montreal from 1997-  
449 2010 and in Toronto from 2003-2019. In contrast, varying weather conditions likely  
450 caused 1 ppb decrease in Quebec from 1995-2019 and in Victoria from 1999-2019.

451

452 The deweathered and original annual average  $NO_2 + O_3$  mixing ratio decreased by 10-  
453 12 ppb in Vancouver from 1986-2019, 10 ppb in Halifax from 2000-2019 and in Toronto  
454 from 2003-2019, 8-10 ppb in Edmonton from 1981-2019 and  $< 6$  ppb in the other cities  
455 (Fig. S5 and Table S4). Based on the simultaneously monitored NO mixing ratios and  
456 the method reportedly used for estimating the primary  $NO_2$  emission (Kurtenbach et al.,  
457 2012; Simon et al., 2015; Casquero-Vera et al., 2019; Xu et al., 2019), the reduced  
458 primary  $NO_2$  emissions likely accounted for only 1-2 ppb decrease in  $NO_2 + O_3$  in the  
459 ten cities and generally acted a minor contributor to the decrease in  $NO_2 + O_3$ .

460

461 *3.4 Trends in deweathered and original  $PM_{2.5}$  mass concentrations*





462 Opposite decadal trends were observed between eastern and western Canadian cities in  
463 the deweathered and original  $PM_{2.5}$  mass concentrations (Table 2, Fig. 3c, d and Fig  
464 S6). In eastern Canadian cities, either decreasing or no significant trends were obtained  
465 in the last two decades. The decreasing trends ( $P < 0.05$ ) were identified in the RF-  
466 deweathered, BRTs-deweathered and original annual average  $PM_{2.5}$  in Montreal from  
467 2005-2019 and in Hamilton from 1998-2019. The overall decreases were only  $2 \mu g m^{-3}$   
468  $^3$  with the decreasing rate of  $0.22-0.25 \mu g m^{-3} year^{-1}$  in Montreal and  $3-4 \mu g m^{-3}$  and  
469  $0.14-0.15 \mu g m^{-3} year^{-1}$  in Hamilton. The decreasing trends ( $P < 0.05$ ) were also  
470 identified in the RF-deweathered and BRTs-deweathered  $PM_{2.5}$  in Toronto from 2000-  
471 2019 with an overall decrease of only  $2 \mu g m^{-3}$  and a decreasing rate of only  $0.10-0.11$   
472  $\mu g m^{-3} year^{-1}$ . However, no significant trend ( $P > 0.05$ ) was identified in the original  
473 annual average  $PM_{2.5}$  in Toronto, implying that the perturbation derived from varying  
474 weather conditions likely cancelled out the mitigation effects of air pollutants. Note that  
475 there were no decreasing trends in the provincial total primary  $PM_{2.5}$  emissions in  
476 Quebec and Ontario during the periods when  $PM_{2.5}$  mass concentration decreased in  
477 the above-mentioned three cities. This was not surprising because the major chemical  
478 components in  $PM_{2.5}$  were derived mainly from secondary sources (Dabek-  
479 Zlotorzynska et al., 2019; Jeong et al., 2020; Wang et al., 2021). The decreasing  
480 provincial emissions of  $SO_2$ ,  $NO_x$  and volatile organic emissions in Quebec and Ontario  
481 likely have reduced the amounts of their oxidized products in  $PM_{2.5}$  (Xing et al., 2015;  
482 Yao and Zhang, 2019, 2020; Feng et al., 2020; Jeong et al., 2020; ECCC, 2021; Wang  
483 et al., 2021, 2022a). No significant trends ( $P > 0.05$ ) were identified in the deweathered  
484 and original  $PM_{2.5}$  concentrations in Halifax from 2008-2018 and in Quebec from 1998-  
485 2019, which need further investigation.

486

487 In western Canadian cities, either increasing or no significant trends were extracted in  
488 the deweathered and original annual average  $PM_{2.5}$  mass concentrations. Increasing  
489 trends ( $P < 0.05$ ) were identified in the RF-deweathered, BRTs-deweathered and original  
490 annual average  $PM_{2.5}$  in Winnipeg from 2001-2018 with an overall increase of only 1-



491  $2 \mu\text{g m}^{-3}$  and an increasing rate of  $0.09\text{-}0.10 \mu\text{g m}^{-3} \text{ year}^{-1}$ . Increasing trends ( $P < 0.05$ )  
492 were identified in the RF-deweathered and original annual average  $\text{PM}_{2.5}$  in Victoria  
493 from 1999-2019 with an overall increase of only  $1 \mu\text{g m}^{-3}$  and an increasing rate of  
494  $0.07\text{-}0.08 \mu\text{g m}^{-3} \text{ year}^{-1}$ , but no significant trend was identified in the BRTs-deweathered  
495 annual average  $\text{PM}_{2.5}$ . An increasing trend was obtained only in the RF-deweathered  
496 annual average  $\text{PM}_{2.5}$  in Vancouver from 2004-2019, and no significant trends were  
497 identified in the BRTs-deweathered and original annual average  $\text{PM}_{2.5}$ . The  
498 inconsistency between the trends extracted from the three different annual average  
499  $\text{PM}_{2.5}$  data series was mostly because of the small magnitudes of the actual interannual  
500 changes and thus the trends, which are on the same order of magnitude as the  
501 methodology uncertainties. Considering the decreasing trends in  $\text{NO}_2$ ,  $\text{CO}$  and  $\text{SO}_2$   
502 mixing ratios discussed above and the reported decreasing trends in secondary chemical  
503 components of  $\text{PM}_{2.5}$  in Western Canada (Wang et al., 2021, 2022a), the increasing  
504 trends in the deweathered and/or original annual average  $\text{PM}_{2.5}$  observed in some  
505 western Canadian cities were likely caused by increased natural emissions, such as from  
506 the increased forest fires in recent years.

507

508 It is noticed that a few spikes always appeared in the BRTs-deweathered  $\text{PM}_{2.5}$   
509 concentrations in the five western Canadian Cities since 2010 (Fig. S6). Most of these  
510 spikes were associated with large-scale wildfire emissions (Littell et al., 2009; Collier  
511 et al., 2016; Landis et al., 2018; Matz et al., 2020). For example, wildfires caused large  
512 and rapid increases in  $\text{PM}_{2.5}$  mass concentration from  $\leq 10 \mu\text{g m}^{-3}$  to  $>400 \mu\text{g m}^{-3}$  in  
513 Edmonton during 10-12 August 1998 and on 30 May 2019 (Fig. S1). During the periods,  
514 the BRTs method predicts the spikes of  $\text{PM}_{2.5}$ . However, the RF method seemingly  
515 failed to learn the wildfire signals and missed in predicting the spikes associated with  
516 largely increased natural emissions.

517

518 To further explore the causes for the different trends in  $\text{PM}_{2.5}$  between eastern and  
519 western Canadian cities, the 95<sup>th</sup>-100<sup>th</sup> percentile  $\text{PM}_{2.5}$  mass concentration data in each



520 year were averaged into annual value and were examined below. The top 5% PM<sub>2.5</sub>  
521 exhibited decreasing trends (P<0.05) in four eastern Canadian cities and no significant  
522 trend (P>0.05) in Halifax (Fig. S7). The decreasing trends further confirmed the  
523 mitigation effects of air pollutants on PM<sub>2.5</sub>. However, annual average PM<sub>2.5</sub> was still  
524 as high as 8.8 µg m<sup>-3</sup> in Hamilton in 2019, 7.0-7.7 µg m<sup>-3</sup> in Quebec, Toronto and  
525 Montreal, and 5.6 µg m<sup>-3</sup> in Halifax. If keeping the same decreasing rates as mentioned  
526 above, it would take another 1-3 decades to lower annual average PM<sub>2.5</sub> by 2-4 µg m<sup>-3</sup>  
527 in order to meet the WHO 2021 guideline.

528

529 No significant trends (P>0.05) were identified in the 95<sup>th</sup>-100<sup>th</sup> percentile PM<sub>2.5</sub> mass  
530 concentrations in the five western Canadian cities. Note that large standard deviation  
531 of the 95<sup>th</sup>-100<sup>th</sup> percentile PM<sub>2.5</sub> mass concentration was found in some years in the  
532 five western cities, but this is not the case in the eastern Canadian cities. The episodic  
533 PM<sub>2.5</sub> events likely canceled out the mitigation effects in the western Canadian cities.  
534 The annual average PM<sub>2.5</sub> were 6.6-6.8 µg m<sup>-3</sup> in 2019 in Winnipeg, Edmonton and  
535 Victoria, which need great additional mitigation efforts in order to reduce to a level  
536 below 5 µg m<sup>-3</sup> in the presence of the episodes caused by natural emissions. Note that  
537 the annual average PM<sub>2.5</sub> was already lower than 5 µg m<sup>-3</sup> in Vancouver, and that the  
538 annual average was 8.4 µg m<sup>-3</sup> at the study site in Calgary in 2014. The value slightly  
539 decreased to 7.6 µg m<sup>-3</sup> in 2019 at another site ~5 km from the study site in Calgary.

540

### 541 *3.5 Trends in AQHI in the ten Canadian cities*

542 Decreasing trends in AQHI were obtained in nine cities (P<0.05), with Calgary as an  
543 only exception (Figs. S9 and S10). The annual average AQHI decreased by 8-29%  
544 during the last two decades, to the levels of 1.8 to 3.0 during 2017-2019 in the nine  
545 cities. In Calgary, the annual averages AQHI narrowed around 3.4±0.2 during 1998-  
546 2010. In the five eastern cities, AQHI above 10 occurred at <0.3% frequency before  
547 2010, but none after 2010. AQHI between 7-10 occurred at <4% frequency before 2010,  
548 and below 0.5% after 2010. In the five western cities, AQHI above 10 occurred at <0.3%



549 frequency, and AQHI between 7-10 occurred at <2% frequency during the last two  
550 decades. Note that AQHI above 10 still occurred at <0.3% frequency even after 2010  
551 because of the large-scale wildfires. In fact, the occurrence frequencies of AQHI  
552 between 7-10 and above 10 were a bit higher after 2010 than before 2010 in Vancouver  
553 and Victoria due to the increased wildfire events in the most recent decade.

554

555 On seasonal average, AQHI above 10 occurred most in summer in most cities, e.g.,  
556 Victoria (1.1%), Vancouver (0.8%), Edmonton (0.7%) and Winnipeg (0.1%) in 2018.  
557 AQHI above 10 also occurred in winter and spring in some cities, e.g., Edmonton (0.3%  
558 in the spring of 2019 and 0.1-0.3% in the winter of 2012-2013) and Winnipeg (0.1% in  
559 the spring of 2018).

560

#### 561 **4. Discussion**

##### 562 *4.1 Trend analysis of O<sub>3</sub> net sinks and sources*

563 As reported in literature, a large fraction of ground-level O<sub>3</sub> at middle-high latitude  
564 zones comes from secondary reactions associated with natural sources (Barrie et al.,  
565 1988; Van Dam et al., 2013; Cooper et al., 2005; Seinfeld and Pandis, 2006; Mitchell  
566 et al., 2021). The natural signal usually has a spring maximum related to stratosphere-  
567 troposphere exchange as well as increasing photochemistry, among other potential  
568 factors (Chan and Vet, 2010; Monks et al., 2015; Strode et al., 2018; Xu et al., 2019).  
569 The contributions from stratosphere-troposphere exchange were approximately 40 ppb,  
570 while the sinks associated with natural and anthropogenic factors in the atmospheric  
571 boundary layer may decrease the ground-level O<sub>3</sub> to levels lower than 40 ppb (Barrie  
572 et al., 1988; Van Dam et al., 2013; Chan and Vet, 2010; Monks et al., 2015; Mitchell et  
573 al., 2021). On the other hand, enhanced tropospheric photochemical reactions under  
574 favorable meteorological conditions may increase the ground-level O<sub>3</sub> to levels higher  
575 than 40 ppb, causing severe O<sub>3</sub> pollution (Monks et al., 2015; Simon et al., 2015;  
576 Seinfeld and Pandis 2006; Xu et al., 2019). Thus, O<sub>3</sub> data with mixing ratios lower and  
577 higher than 40 ppb were analyzed separately below, with the former case representing



578 net O<sub>3</sub> sinks occurring in the atmospheric boundary layer and the latter one representing  
579 net O<sub>3</sub> sources occurring therein (Table 3).

580

581 In the cases with O<sub>3</sub> mixing ratios  $\geq 40$  ppb, the deweathered and original values,  
582 however, exhibited decreasing trends ( $P < 0.05$ ) in all of the five eastern cities and two  
583 western cities (Victoria and Vancouver) (Figs. 4 and S8 and Table 3). The overall  
584 decreases in O<sub>3</sub> with mixing ratios  $\geq 40$  ppb were 2 ppb in Halifax from 2000-2017, in  
585 Montreal and Quebec from 1995-2019, and in Victoria from 1999-2019 (figure not  
586 provided), 4 ppb in Toronto from 2003-2019, 5-6 ppb in Hamilton from 1987-2019, and  
587 12 ppb in Vancouver from 1986-2019 (but only 2 ppb from 2000-2019). Again, a few  
588 spikes and troughs occurred in the BRTs-deweathered values possibly because of  
589 unpredictably increased and decreased emissions of O<sub>3</sub> precursors, respectively. In the  
590 cases with NO<sub>2</sub>+O<sub>3</sub> mixing ratios  $\geq 40$  ppb, the decreasing trends were obtained in all  
591 of the ten cities. These results further implied that the tropospheric photochemical  
592 formation of O<sub>3</sub> likely reduced in seven of the ten cities during the last two to three  
593 decades.

594

595 In the cases with O<sub>3</sub> with mixing ratios  $\geq 40$  ppb in the remaining three western cities,  
596 the decreasing trends ( $P < 0.05$ ) were obtained in the BRTs-deweathered and original  
597 values and no significant trend ( $P > 0.05$ ) in the RF-deweathered values in Winnipeg;  
598 the decreasing trend was obtained only in the original values in Calgary; and no  
599 significant trends in the deweathered and original values in Edmonton. These trend  
600 results implied that the responses of the fraction of O<sub>3</sub> to emission reductions of its  
601 precursors were too weak to be confirmed, especially in the presence of perturbation  
602 from varying weather conditions.

603

604 In the cases with O<sub>3</sub> mixing ratios  $< 40$  ppb, the trends were almost the same as those  
605 from using the full dataset of O<sub>3</sub> mixing ratios. This consistency suggested that the  
606 increasing trends in O<sub>3</sub> mixing ratio in the nine Canadian cities were mainly due to the



607 reduced O<sub>3</sub> sinks.

608

609 *4.2 The perturbation from large-scale wildfires on PM<sub>2.5</sub> trend in western Canadian*  
610 *cities*

611 Wildfire emissions become important contributors to air pollution in North America  
612 with global warming and increased extreme weather conditions such as heatwaves and  
613 severe droughts (Andreae and Merlet, 2001; Littell et al., 2009; Marlon et al., 2013;  
614 Barbero et al., 2015; Abatzoglou and Williams, 2016; Randerson et al., 2017; Mardi et  
615 al., 2021). For example, Meng et al. (2019) estimated that wildfires accounted for 17.1%  
616 of the total population-weighted exposure to PM<sub>2.5</sub> for Canadians during 2013-2015  
617 and 2017-2018. Their modeling results also showed that wildfires dominantly  
618 contributed to the population-weighted exposure to PM<sub>2.5</sub> in northern Canada (59%)  
619 and western Canada (18%), which was not surprising because large wildfires can  
620 rapidly increase hourly PM<sub>2.5</sub> mass concentration from a few  $\mu\text{g m}^{-3}$  to  $>400 \mu\text{g m}^{-3}$   
621 (Landis et al., 2018 and Fig. S1). The estimated annual economic cost attributable to  
622 PM<sub>2.5</sub> pollution reached \$410M-\$1.8B for acute health impacts and \$4.3B-\$19B for  
623 chronic health impacts in western Canada (Landis et al., 2018; Matz et al., 2020). In the  
624 U.S., wildfire emissions were reported to account for up to 25% of annual primary  
625 PM<sub>2.5</sub> emissions (U.S. EPA, 2014).

626

627 Due to the wide occurrence of small-scale wildfires, most of the emitted air pollutants  
628 from these sources and subsequent long-range transport can be considered as natural  
629 background pollution. The key issue is to quantify the abnormally increased  
630 contributions from large-scale wildfires to annual average PM<sub>2.5</sub> in each year and their  
631 perturbations on long-term trends in PM<sub>2.5</sub>. Using the method described in Section 2,  
632 the perturbation contributions in Winnipeg were estimated to be around  $0.5 \pm 0.4 \mu\text{g m}^{-3}$   
633 <sup>3</sup> in 2001-2018, with larger values of 1.1-1.3  $\mu\text{g m}^{-3}$  associated with large-scale wildfires  
634 in 2002, 2012 and 2018 (Fig. 5a). The larger perturbation contributions in 2012 and  
635 2018 indeed led to an increasing trend in PM<sub>2.5</sub> from 2001-2018 in this city (Table 2).



636 The perturbation contributions were, however, smaller than  $0.2 \mu\text{g m}^{-3}$  in 2001, 2003,  
637 2005, 2006, 2008, 2009, 2014 and 2017, and such small values may be related to  
638 varying weather conditions rather than large-scale wildfires.

639

640 In Edmonton, the perturbation contributions were around  $1.0 \pm 0.9 \mu\text{g m}^{-3}$  in 1998-2019  
641 (Fig. 5b). However, the largest contribution was  $3.0 \mu\text{g m}^{-3}$  in 1998, followed by  $2.4 \mu\text{g}$   
642  $\text{m}^{-3}$  in 2018 and  $2.1 \mu\text{g m}^{-3}$  in 2004, respectively, because of large-scale wildfires. The  
643 perturbation contributions from large-scale wildfires were large enough to cancel out  
644 the mitigation effect of air pollutants on annual averages of  $\text{PM}_{2.5}$  in Edmonton. In  
645 Calgary, the perturbation contributions were around  $1.2 \pm 0.7 \mu\text{g m}^{-3}$  in 1998-2013,  
646 depending on if large-scale wildfires occurred in any particular year. For example, the  
647 perturbation contributions were smaller than  $0.2 \mu\text{g m}^{-3}$  in 1999, 2007 and 2013, while  
648 the contributions reached  $2.2$ - $2.3 \mu\text{g m}^{-3}$  in 1998 and 2010.

649

650 In Victoria, the perturbation contributions were around  $0.7 \pm 0.2 \mu\text{g m}^{-3}$  in 1998-2019.,  
651 The perturbation contribution in each year was, however, larger than  $0.4 \mu\text{g m}^{-3}$ ,  
652 suggesting that the wildfires were always important contributors. In Vancouver, the  
653 perturbation contributions largely decreased to  $0.3 \pm 0.5 \mu\text{g m}^{-3}$  in 2004-2019. However,  
654 the maximum value still reached  $1.7 \mu\text{g m}^{-3}$  in 2017, followed by  $1.4 \mu\text{g m}^{-3}$  in 2018  
655 and  $0.5 \mu\text{g m}^{-3}$  in 2015. The large perturbation likely overwhelmed or canceled out the  
656 effects of emission reductions on annual average  $\text{PM}_{2.5}$ .

657

## 658 **5. Conclusions**

659 Through analysis of deweathered and original annual average concentrations of criteria  
660 air pollutants measured in ten major cities in Canada during the last 2-3 decades, we  
661 found 1) decreasing trends in  $\text{NO}_2$ ,  $\text{CO}$  and  $\text{SO}_2$  mainly due to reduced primary  
662 emissions across Canada, except no significant trend in  $\text{CO}$  in Montreal; 2) increasing  
663 trends in  $\text{O}_3$  mainly due to the reduced titration effect across Canada, except no  
664 significant trend in  $\text{O}_3$  in Halifax; and 3) roughly opposite trends in  $\text{PM}_{2.5}$  between



665 eastern and western Canada, resulted from the combined effects of emission reductions  
666 and the occurrence of large-scale wildfires.

667

668 Combining results from the deweathered and original annual average data together, the  
669 overall percentage decrease in NO<sub>2</sub> during the last 2-3 decades varied by 37%-62%,  
670 and the annual decreasing rates between the 10 cities varied from 0.31 ppb year<sup>-1</sup> to  
671 0.74 ppb year<sup>-1</sup>. The overall percentage decrease in CO varied from 57% to 92% and  
672 the annual decreasing rate ranged from 0.010 ppm year<sup>-1</sup> to 0.076 ppm year<sup>-1</sup> between  
673 nine cities. The corresponding numbers for SO<sub>2</sub> are from 23% to 93% and from 0.04  
674 ppb year<sup>-1</sup> to 0.63 ppb year<sup>-1</sup> among 10 cities.

675

676 Using the full data set of annual average O<sub>3</sub> mixing ratios, the reduced titration effect  
677 was detected, which overwhelmed or cancelled out the effects of emission reduction of  
678 its gaseous precursors. If only considering cases with O<sub>3</sub> ≥ 40 ppb, annual average O<sub>3</sub>  
679 decreased by 2-4 ppb in most cities during the past two-three decades, but not in  
680 Calgary and Edmonton, and no consistent decreasing trend was identified in Winnipeg,  
681 implying that the mitigation effects of air pollutants on O<sub>3</sub> were too weak to be  
682 confirmed.

683

684 The mitigation effects on PM<sub>2.5</sub> were detected on the basis of the identified decreasing  
685 trends in three of the five eastern cities regardless of using original or deweathered  
686 annual average data, but this is not the case in the other two eastern cities. In the five  
687 western cities, the perturbation mainly from large-scale wildfires greatly affected  
688 original annual average PM<sub>2.5</sub> in some years and cancelled out the mitigation effects,  
689 leading to no decreasing trends and in some cases even with increasing trends.

690

691 Excluding Calgary, the annual average AQHI showed a significant decrease by 8-29%  
692 during the last two decades to levels between 1.8 and 3.0 in 2017-2019. However, large-  
693 scale wildfire events still occasionally caused AQHI to a level of above 10 (very high





694 risk) (<0.3% frequency) in western Canadian cities after 2010. Thus, large-scale  
695 wildfires have become a key factor in causing severe air pollution in Canadian cities,  
696 as was seen in the most recent very large-scale wildfires occurred in Canada from the  
697 later spring to the earlier summer in 2023 that resulted in severe air pollution across  
698 Canada and New York through long-range transport. Urgent work should be conducted  
699 for assessing the impacts of large-scale wildfires on human health and climate change,  
700 besides investigating their occurrence and control mechanisms and transport pathways.  
701 In-depth studies are also needed to explore the causes of the non-decreasing trends in  
702 O<sub>3</sub> with mixing ratios  $\geq 40$  ppb in some western Canadian cities, results from which are  
703 critical for making future control policies.

704

705 **Acknowledgement.** We greatly appreciate all the personnel of the NAPS Partners  
706 who operate the sites across Canada and collect the field samples, and the staff of the  
707 Analysis and Air Quality section in Ottawa for the laboratory chemical analyses and  
708 QA/QC of the data used in the present study. NPRI/APEI groups are also  
709 acknowledged for their efforts in generating emissions data across Canada.

710

711 *Data availability.* the data used in this paper are downloadable from  
712 <https://open.canada.ca/data/en/dataset/1b36a356-defd-4813-acea-47bc3abd859b>) and  
713 [https://www.canada.ca/en/environment-climate-change/services/environmental-](https://www.canada.ca/en/environment-climate-change/services/environmental-indicators/air-pollutant-emissions.html)  
714 [indicators/air-pollutant-emissions.html](https://www.canada.ca/en/environment-climate-change/services/environmental-indicators/air-pollutant-emissions.html).

715

716 *Author contributions.* XY and LZ designed the research, conducted analysis, and  
717 prepared the manuscript.

718

719 *Competing interests.* One of the (co-)authors is a member of the editorial board of ACP.

720

## 721 **References**

722 Abatzoglou, J. T. and Williams, A. P.: Impact of anthropogenic climate change on  
723 wildfire across western US forests, Proc. Natl. Acad. Sci. USA., 113, 11770-11775,  
724 <https://doi.org/10.1073/pnas.1607171113>, 2016.



- 725 Al-Abadleh, H. A., Lysy, M., Neil, L., Patel, P., Mohammed, W., and Khalaf, Y.:  
726 Rigorous quantification of statistical significance of the COVID-19 lockdown effect  
727 on air quality: The case from ground-based measurements in Ontario, Canada, *J.*  
728 *Hazard. Mater.*, 413, 125445, <https://doi.org/10.1016/j.jhazmat.2021.125445>, 2021.
- 729 Andreae, M. O. and Merlet, P.: Emission of trace gases and aerosols from biomass  
730 burning, *Global. Biogeochem. Cy.*, 15, 955-966,  
731 <https://doi.org/10.1029/2000GB001382>, 2001.
- 732 Astitha, M., Luo, H., Rao, S. T., Hogrefe, C., Mathur, R., and Kumar, N.: Dynamic  
733 Evaluation of Two Decades of WRF-CMAQ Ozone Simulations over the  
734 Contiguous United States, *Atmos. Environ.* (1994), 164, 102-116,  
735 <https://doi.org/10.1016/j.atmosenv.2017.05.020>, 2017.
- 736 Aziz, J. J., Ling, M., Rifai, H. S., Newell, C. J., and Gonzales, J. R.: MAROS: a decision  
737 support system for optimizing monitoring plans, *Ground. Water.*, 41, 355-367,  
738 <https://doi.org/10.1111/j.1745-6584.2003.tb02605.x>, 2003.
- 739 Barbero, R., Abatzoglou, J. T., Larkin, N. K., Kolden, C. A., and Stocks, B.: Climate  
740 change presents increased potential for very large fires in the contiguous United  
741 States, *Int. J. Wildland. Fire.*, 24, <https://doi.org/10.1071/WF15083>, 2015.
- 742 Bari, M.A., Kindzierski, W.B. Eight-year (2007–2014) trends in ambient fine  
743 particulate matter (PM<sub>2.5</sub>) and its chemical components in the Capital Region of  
744 Alberta, Canada. *Environment Int.* 91, 122–132,  
745 <http://doi:10.1016/j.envint.2016.02.033>, 2016.
- 746 Barrie, L. A., Bottenheim, J. W., Schnell, R. C., Crutzen, P. J., and Rasmussen, R. A.:  
747 Ozone destruction and photochemical reactions at polar sunrise in the lower Arctic  
748 atmosphere, *Nature*, 334, 138-141, <https://doi.org/10.1038/334138A0>, 1988.
- 749 Bowdalo, D., Petetin, H., Jorba, O., Guevara, M., Soret, A., Bojovic, D., Terrado, M.,  
750 Querol, X., and Pérez García-Pando, C.: Compliance with 2021 WHO air quality  
751 guidelines across Europe will require radical measures, *Environ. Res. Lett.*, 17,  
752 <https://doi.org/10.1088/1748-9326/ac44c7>, 2022.
- 753 Carslaw, D. C. and Taylor, P. J.: Analysis of air pollution data at a mixed source location  
754 using boosted regression trees, *Atmos. Environ.*, 43, 3563-3570,  
755 <https://doi.org/10.1016/j.atmosenv.2009.04.001>, 2009.
- 756 Carslaw, D. C. and Ropkins, K.: openair — An R package for air quality data analysis,  
757 *Environ. Modell. Softw.*, 27-28, 52-61,



- 758 <https://doi.org/10.1016/j.envsoft.2011.09.008>, 2012.
- 759 Carslaw, D. C.: Worldmet: Import Surface Meteorological Data from NOAA Integrated  
760 Surface Database (ISD), R package version 0.9.5, [https://cran.r-](https://cran.r-project.org/package=worldmet)  
761 [project.org/package=worldmet](https://cran.r-project.org/package=worldmet). 2021.
- 762 Casquero-Vera, J. A., Lyamani, H., Titos, G., Borrás, E., Olmo, F. J., and Alados-  
763 Arboledas, L.: Impact of primary NO<sub>2</sub> emissions at different urban sites exceeding  
764 the European NO<sub>2</sub> standard limit, *Sci. Total. Environ.*, 646, 1117-1125,  
765 <https://doi.org/10.1016/j.scitotenv.2018.07.360>, 2019.
- 766 Chan, E. and Vet, R. J.: Baseline levels and trends of ground level ozone in Canada and  
767 the United States, *Atmos. Chem. Phys.*, 10, 8629-8647, [https://doi.org/10.5194/acp-](https://doi.org/10.5194/acp-10-8629-2010)  
768 [10-8629-2010](https://doi.org/10.5194/acp-10-8629-2010), 2010.
- 769 Collier, S., Zhou, S., Onasch, T. B., Jaffe, D. A., Kleinman, L., Sedlacek, A. J., 3rd,  
770 Briggs, N. L., Hee, J., Fortner, E., Shilling, J. E., Worsnop, D., Yokelson, R. J.,  
771 Parworth, C., Ge, X., Xu, J., Butterfield, Z., Chand, D., Dubey, M. K., Pekour, M.  
772 S., Springston, S., and Zhang, Q.: Regional Influence of Aerosol Emissions from  
773 Wildfires Driven by Combustion Efficiency: Insights from the BBOP Campaign,  
774 *Environ. Sci. Technol.*, 50, 8613-8622, <https://doi.org/10.1021/acs.est.6b01617>,  
775 2016.
- 776 Cooper, O. R.: A springtime comparison of tropospheric ozone and transport pathways  
777 on the east and west coasts of the United States, *J. Geophys. Res.*, 110,  
778 <https://doi.org/10.1029/2004JD005183>, 2005.
- 779 Dabek-Zlotorzynska, E., Celó, V., Ding, L., Herod, D., Jeong, C.-H., Evans, G., and  
780 Hilker, N.: Characteristics and sources of PM<sub>2.5</sub> and reactive gases near roadways  
781 in two metropolitan areas in Canada, *Atmos. Environ.*, 218,  
782 <https://doi.org/10.1016/j.atmosenv.2019.116980>, 2019.
- 783 Dabek-Zlotorzynska, E., Dann, T. F., Kalyani Martinelango, P., Celó, V., Brook, J. R.,  
784 Mathieu, D., Ding, L., and Austin, C. C.: Canadian National Air Pollution  
785 Surveillance (NAPS) PM<sub>2.5</sub> speciation program: Methodology and PM<sub>2.5</sub> chemical  
786 composition for the years 2003–2008, *Atmos. Environ.*, 45, 673-686,  
787 <https://doi.org/10.1016/j.atmosenv.2010.10.024>, 2011.
- 788 Dai, Q., Hou, L., Liu, B., Zhang, Y., Song, C., Shi, Z., Hopke, P. K., and Feng, Y.: Spring  
789 Festival and COVID-19 Lockdown: Disentangling PM Sources in Major Chinese  
790 Cities, *Geophys. Res. Lett.*, 48, e2021GL093403,



791 <https://doi.org/10.1029/2021gl093403>, 2021.

792 ECCC, Environment and Climate Change Canada: Canadian Environmental  
793 Sustainability Indicators: Air pollutant emissions, available at:  
794 [https://www.canada.ca/en/environment-climate-change/services/environmental-  
795 indicators/air-pollutant-emissions.html](https://www.canada.ca/en/environment-climate-change/services/environmental-<br/>795 indicators/air-pollutant-emissions.html), last access: 20 October 2023.

796 ECCC, Environment and Climate Change Canada: (2023) Canadian Environmental  
797 Sustainability Indicators: Air Quality. Available at:  
798 [www.canada.ca/en/environment-climate-change/services/environmental-  
799 indicators/air-quality.html](http://www.canada.ca/en/environment-climate-change/services/environmental-<br/>799 indicators/air-quality.html), last access 20 October 2023.

800 Feng, J., Chan, E., Vet, R. Air quality in the eastern United States and Eastern Canada  
801 for 1990–2015: 25 years of change in response to emission reductions of SO<sub>2</sub> and  
802 NO<sub>x</sub> in the region. *Atmos. Chem. Phys.*, 20, 3107–3134,  
803 <https://doi.org/10.5194/acp-20-3107-2020>

804 Foley, K. M., Hogrefe, C., Pouliot, G., Possiel, N., Roselle, S. J., Simon, H., and Timin,  
805 B.: Dynamic evaluation of CMAQ part I: Separating the effects of changing  
806 emissions and changing meteorology on ozone levels between 2002 and 2005 in the  
807 eastern US, *Atmos. Environ.*, 103, 247–255,  
808 <https://doi.org/10.1016/j.atmosenv.2014.12.038>, 2015.

809 Grange, S. K. and Carslaw, D. C.: Using meteorological normalisation to detect  
810 interventions in air quality time series, *Sci. Total. Environ.*, 653, 578–588,  
811 <https://doi.org/10.1016/j.scitotenv.2018.10.344>, 2019.

812 Grange, S. K., Carslaw, D. C., Lewis, A. C., Boleti, E., and Hueglin, C.: Random forest  
813 meteorological normalisation models for Swiss PM<sub>10</sub> trend analysis, *Atmos. Chem.  
814 Phys.*, 18, 6223–6239, <https://doi.org/10.5194/acp-18-6223-2018>, 2018.

815 Griffin, D., McLinden, C. A., Racine, J., Moran, M. D., Fioletov, V., Pavlovic, R.,  
816 Mashayekhi, R., Zhao, X., and Eskes, H.: Assessing the Impact of Corona-Virus-19  
817 on Nitrogen Dioxide Levels over Southern Ontario, Canada, *Remote Sens-Basel*,  
818 12, <https://doi.org/10.3390/rs12244112>, 2020.

819 Health Canada. 2021. Health impacts of air pollution in Canada – Estimate of morbidity  
820 and premature mortality outcomes – 2021 report. Government of Canada. ISBN  
821 978-0-660-37331-7. 56 pp. [https://www.canada.ca/content/dam/hc-  
822 sc/documents/services/publications/healthy-living/2021-health-effects-indoor-air-  
823 pollution/hia-report-eng.pdf](https://www.canada.ca/content/dam/hc-<br/>822 sc/documents/services/publications/healthy-living/2021-health-effects-indoor-air-<br/>823 pollution/hia-report-eng.pdf)



- 824 Jeong, C.-H., Traub, A., Huang, A., Hilker, N., Wang, J. M., Herod, D., Dabek-  
825 Zlotorzynska, E., Celò, V., and Evans, G. J.: Long-term analysis of PM<sub>2.5</sub> from 2004  
826 to 2017 in Toronto: Composition, sources, and oxidative potential, *Environ. Pollut.*,  
827 263, <https://doi.org/10.1016/j.envpol.2020.114652>, 2020.
- 828 Kampata, J. M., Parida, B. P., and Moalafhi, D. B.: Trend analysis of rainfall in the  
829 headstreams of the Zambezi River Basin in Zambia, *Phys. Chem. Earth.*, 33, 621-  
830 625, <https://doi.org/10.1016/j.pce.2008.06.012>, 2008.
- 831 Kurtenbach, R., Kleffmann, J., Niedojadlo, A., and Wiesen, P.: Primary NO<sub>2</sub> emissions  
832 and their impact on air quality in traffic environments in Germany, *Environ. Sci.*  
833 *Eur.*, 24, <https://doi.org/10.1186/2190-4715-24-21>, 2012.  
834 <https://doi.org/10.1016/j.envpol.2020.115900>, 2021.
- 835 Landis, M. S., Edgerton, E. S., White, E. M., Wentworth, G. R., Sullivan, A. P., and  
836 Dillner, A. M.: The impact of the 2016 Fort McMurray Horse River Wildfire on  
837 ambient air pollution levels in the Athabasca Oil Sands Region, Alberta, Canada,  
838 *Sci. Total Environ.*, 618, 1665-1676,  
839 <https://doi.org/10.1016/j.scitotenv.2017.10.008>, 2018.
- 840 Lin, Y., Zhang, L., Fan, Q., Meng, H., Gao, Y., Gao, H., and Yao, X.: Decoupling  
841 impacts of weather conditions on interannual variations in concentrations of criteria  
842 air pollutants in south China—constraining analysis uncertainties by using multiple  
843 analysis tools, *Atmos. Chem. Phys.*, 22, 16073–16090, [https://doi.org/10.5194/acp-](https://doi.org/10.5194/acp-22-16073-2022)  
844 [22-16073-2022](https://doi.org/10.5194/acp-22-16073-2022), 2022
- 845 Littell, J. S., McKenzie, D., Peterson, D. L., and Westerling, A. L.: Climate and wildfire  
846 area burned in western U.S. ecoprovinces, 1916-2003, *Ecol. Appl.*, 19, 1003-1021,  
847 <https://doi.org/10.1890/07-1183.1>, 2009.
- 848 Lovric, M., Pavlovic, K., Vukovic, M., Grange, S. K., Haberl, M., and Kern, R.:  
849 Understanding the true effects of the COVID-19 lockdown on air pollution by  
850 means of machine learning, *Environ. Pollut.*, 274, 115900.
- 851 Ma, R., Ban, J., Wang, Q., Zhang, Y., Yang, Y., He, M. Z., Li, S., Shi, W., and Li, T.:  
852 Random forest model based fine scale spatiotemporal O<sub>3</sub> trends in the Beijing-  
853 Tianjin-Hebei region in China, 2010 to 2017, *Environ. Pollut.*, 276, 116635,  
854 <https://doi.org/10.1016/j.envpol.2021.116635>, 2021.
- 855 Mallet, M. D.: Meteorological normalisation of PM<sub>10</sub> using machine learning reveals  
856 distinct increases of nearby source emissions in the Australian mining town of



- 857 Moranbah, Atmos. Pollut. Res., 12, 23-35,  
858 <https://doi.org/10.1016/j.apr.2020.08.001>, 2021.
- 859 Mardi, A. H., Dadashazar, H., Painemal, D., Shingler, T., Seaman, S. T., Fenn, M. A.,  
860 Hostetler, C. A., and Sorooshian, A.: Biomass Burning Over the United States East  
861 Coast and Western North Atlantic Ocean: Implications for Clouds and Air Quality,  
862 J. Geophys. Res.-Atmos., 126, <https://doi.org/doi:10.1029/2021JD034916>, 2021.
- 863 Marlon, J. R., Bartlein, P. J., Daniau, A.-L., Harrison, S. P., Maezumi, S. Y., Power, M.  
864 J., Tinner, W., and Vanni re, B.: Global biomass burning: a synthesis and review of  
865 Holocene paleofire records and their controls, Quaternary. Sci. Rev., 65, 5-25,  
866 <https://doi.org/10.1016/j.quascirev.2012.11.029>, 2013.
- 867 Matz, C. J., Egyed, M., Xi, G., Racine, J., Pavlovic, R., Rittmaster, R., Henderson, S.  
868 B., and Stieb, D. M.: Health impact analysis of PM<sub>2.5</sub> from wildfire smoke in  
869 Canada (2013-2015, 2017-2018), Sci. Total. Environ., 725, 138506,  
870 <https://doi.org/10.1016/j.scitotenv.2020.138506>, 2020.
- 871 Meng, J., Martin, R. V., Li, C., van Donkelaar, A., Tzompa-Sosa, Z. A., Yue, X., Xu, J.  
872 W., Weagle, C. L., and Burnett, R. T.: Source Contributions to Ambient Fine  
873 Particulate Matter for Canada, Environ. Sci. Technol., 53, 10269-10278,  
874 <https://doi.org/10.1021/acs.est.9b02461>, 2019.
- 875 Mitchell, M., Wiacek, A., and Ashpole, I.: Surface ozone in the North American  
876 pollution outflow region of Nova Scotia: Long-term analysis of surface  
877 concentrations, precursor emissions and long-range transport influence, Atmos.  
878 Environ., 261, <https://doi.org/10.1016/j.atmosenv.2021.118536>, 2021.
- 879 Monks, P. S., Archibald, A. T., Colette, A., Cooper, O., Coyle, M., Derwent, R., Fowler,  
880 D., Granier, C., Law, K. S., Mills, G. E., Stevenson, D. S., Tarasova, O., Thouret,  
881 V., von Schneidmesser, E., Sommariva, R., Wild, O., and Williams, M. L.:  
882 Tropospheric ozone and its precursors from the urban to the global scale from air  
883 quality to short-lived climate forcer, Atmos. Chem. Phys., 15, 8889-8973,  
884 <https://doi.org/10.5194/acp-15-8889-2015>, 2015.
- 885 Munir, S., Luo, Z., and Dixon, T.: Comparing different approaches for assessing the  
886 impact of COVID-19 lockdown on urban air quality in Reading, UK, Atmos. Res.,  
887 261, 105730, <https://doi.org/10.1016/j.atmosres.2021.105730>, 2021.
- 888 Pappin, A. J., Hakami, A., Blagden, P., Nasari, M., Szyszkowicz, M., and Burnett, R.  
889 T.: Health benefits of reducing NO<sub>x</sub> emissions in the presence of epidemiological



890 and atmospheric nonlinearities, *Environ. Res. Lett.*, 11,  
891 <https://doi.org/10.1088/1748-9326/11/6/064015>, 2016.

892 Randerson, J.T., G.R. van der Werf, L. Giglio, G.J. Collatz, and P.S. Kasibhatla. 2017.  
893 Global Fire Emissions Database, Version 4.1 (GFEDv4). ORNL DAAC, Oak Ridge,  
894 Tennessee, USA. <https://doi.org/10.3334/ORNLDAAAC/1293>.

895 Ren, S., Stroud, C., Belair, S., Leroyer, S., Munoz-Alpizar, R., Moran, M., Zhang, J.,  
896 Akingunola, A., and Makar, P.: Impact of Urbanization on the Predictions of Urban  
897 Meteorology and Air Pollutants over Four Major North American Cities,  
898 *Atmosphere-Basel*, 11, <https://doi.org/10.3390/atmos11090969>, 2020.

899 Seinfeld, J.H. and Pandis, S.N. (2006) *Atmospheric Chemistry and Physics: From Air*  
900 *Pollution to Climate Change*. 2nd Edition, John Wiley & Sons, New York.

901 Shi, X. and Brasseur, G. P.: The Response in Air Quality to the Reduction of Chinese  
902 Economic Activities During the COVID-19 Outbreak, *Geophys. Res. Lett.*, 47,  
903 e2020GL088070, <https://doi.org/10.1029/2020GL088070>, 2020.

904 Shi, Z., Song, C., Liu, B., Lu, G., Xu, J., Van Vu, T., Elliott, R. J. R., Li, W., Bloss, W.  
905 J., and Harrison, R. M.: Abrupt but smaller than expected changes in surface air  
906 quality attributable to COVID-19 lockdowns, *Sci. Adv. Mater.*, 7,  
907 <https://doi.org/10.1126/sciadv.abd6696>, 2021.

908 Sicard, P., De Marco, A., Agathokleous, E., Feng, Z., Xu, X., Paoletti, E., Rodriguez, J.  
909 J. D., and Calatayud, V.: Amplified ozone pollution in cities during the COVID-19  
910 lockdown, *Sci. Total. Environ.*, 735, 139542,  
911 <https://doi.org/10.1016/j.scitotenv.2020.139542>, 2020.

912 Simon, H., Reff, A., Wells, B., Xing, J., and Frank, N.: Ozone trends across the United  
913 States over a period of decreasing NO<sub>x</sub> and VOC emissions, *Environ. Sci. Technol.*,  
914 49, 186-195, <https://doi.org/10.1021/es504514z>, 2015.

915 Stieb, D.M.; Burnett, R.T.; Smith-Doiron, M.; Brion, O.; Shin, H.H.; Economou, V.: A  
916 new multipollutant, no-threshold air quality health index based on short-term  
917 associations observed in daily time-series analyses, *J. Air Waste Manag. Assoc.* 58,  
918 435–450, <https://doi.org/10.3155/1047-3289.58.3.435>, 2008.

919 Strode, S. A., Ziemke, J. R., Oman, L. D., Lamsal, L. N., Olsen, M. A., and Liu, J.:  
920 Global changes in the diurnal cycle of surface ozone, *Atmos. Environ.*, 199, 323-  
921 333, <https://doi:10.1016/j.atmosenv.2018.11.028>, 2019.

922 To T., Shen S., Atenafu E.G., Guan J., McLimont S., Stocks B.: The Air Quality Health



- 923 Index and asthma morbidity: A population-based study. *Environ Health Perspect.*  
924 121:46–52; <https://ehp.niehs.nih.gov/doi/10.1289/ehp.1104816>, 2013.
- 925 Van Dam, B., Helmig, D., Burkhardt, J. F., Obrist, D., and Oltmans, S. J.: Springtime  
926 boundary layer O<sub>3</sub> and GEM depletion at Toolik Lake, Alaska, *J. Geophys. Res.-*  
927 *Atmos.*, 118, 3382-3391, <https://doi.org/10.1002/jgrd.50213>, 2013.
- 928 Vu, T. V., Shi, Z., Cheng, J., Zhang, Q., He, K., Wang, S., and Harrison, R. M.:  
929 Assessing the impact of clean air action on air quality trends in Beijing using a  
930 machine learning technique, *Atmos. Chem. Phys.*, 19, 11303-11314,  
931 <https://doi.org/10.5194/acp-19-11303-2019>, 2019.
- 932 Wang, H., Zhang, L., Yao, X., Cheng, I., and Dabek-Zlotorzynska, E.: Identification of  
933 decadal trends and associated causes for organic and elemental carbon in PM<sub>2.5</sub> at  
934 Canadian urban sites, *Environ. Int.*, 159, 107031,  
935 <https://doi.org/10.1016/j.envint.2021.107031>, 2022a.
- 936 Wang, H.; Lu, X.; Jacob, D.J.; Cooper, O.R.; Chang, K.L.; Li, K.; Gao, M.; Liu, Y.;  
937 Sheng, B.; Wu, K.; Wu, T.; Zhang, J.; Sauvage, B.; Nédélec, P.; Blot, R.; Fan, S.  
938 Global tropospheric ozone trends, attributions, and radiative impacts in 1995–2017:  
939 an integrated analysis using aircraft (IAGOS) observations, ozonesonde, and multi-  
940 decadal chemical model simulations. *Atmos. Chem. Phys.*, 22, 13753-13782,  
941 <https://doi.org/10.5194/acp-22-13753-2022>, 2022b.
- 942 Wang, H., Zhang, L., Cheng, I., Yao, X., and Dabek-Zlotorzynska, E.: Spatiotemporal  
943 trends of PM<sub>2.5</sub> and its major chemical components at urban sites in Canada, *J.*  
944 *Environ. Sci-China.*, 103, 1-11, <https://doi.org/10.1016/j.jes.2020.09.035>, 2021.
- 945 Wang, Y., Wen, Y., Wang, Y., Zhang, S., Zhang, K. M., Zheng, H., Xing, J., Wu, Y., and  
946 Hao, J.: Four-Month Changes in Air Quality during and after the COVID-19  
947 Lockdown in Six Megacities in China, *Environ. Sci. Tech. Let.*, 7, 802-808,  
948 <https://doi.org/10.1021/acs.estlett.0c00605>, 2020.
- 949 WHO, WHO global air quality guidelines: Particulate matter (PM<sub>2.5</sub> and PM<sub>10</sub>), ozone,  
950 nitrogen dioxide, sulfur dioxide and carbon monoxide, ISBN-13: 978-92-4-003421-  
951 1, <https://www.who.int/publications/i/item/9789240034228>, 2021.
- 952 Xing, J., Mathur, R., Pleim, J., Hogrefe, C., Gan, C. M., Wong, D. C., Wei, C., Gilliam,  
953 R., and Pouliot, G.: Observations and modeling of air quality trends over 1990–  
954 2010 across the Northern Hemisphere: China, the United States and Europe, *Atmos.*  
955 *Chem. Phys.*, 15, 2723-2747, <https://doi.org/10.5194/acp-15-2723-2015>, 2015.





- 956 Xu, X., Zhang, T., and Su, Y.: Temporal variations and trend of ground-level ozone  
957 based on long-term measurements in Windsor, Canada, *Atmos. Chem. Phys.*, 19,  
958 7335-7345, <https://doi.org/10.5194/acp-19-7335-2019>, 2019.
- 959 Yao, J., Stieb, D.M., Taylor, E., Henderson, S.: Assessment of the air quality health  
960 index (AQHI) and four alternate AQHI-Plus amendments for wildfire seasons in  
961 British Columbia. *Can J Public Health* 111, 96–106.  
962 <https://doi.org/10.17269/s41997-019-00237-w>, 2020.
- 963 Yao, X. and Zhang, L.: Causes of large increases in atmospheric ammonia in the last  
964 decade across North America. *ACS Omega*, 11, 4(26), 22133-22142, <https://doi.org/10.1021/acsomega.9b03284>, 2019.
- 966 Yao, X. and Zhang, L.: Decoding long-term trends in the wet deposition of sulfate,  
967 nitrate, and ammonium after reducing the perturbation from climate anomalies,  
968 *Atmos. Chem. Phys.*, 20, 721-733, <https://doi.org/10.5194/acp-20-721-2020>, 2020.
- 969 Zhang, T., Xu, X., and Su, Y.: Long-term measurements of ground-level ozone in  
970 Windsor, Canada and surrounding areas, *Chemosphere*, 294, 133636,  
971 <https://doi.org/10.1016/j.chemosphere.2022.133636>, 2022.
- 972 Zhou, Y., Mao, H., Demerjian, K., Hogrefe, C., and Liu, J.: Regional and Hemispheric  
973 Influences on Temporal Variability in Baseline Carbon Monoxide and Ozone over  
974 the Northeast US, *Atmos. Environ.* 164, 309-324,  
975 <http://dx.doi.org/10.1016/j.atmosenv.2017.06.017>, 2017.



Table 1. Correlations between deweathered NO<sub>2</sub> mixing ratios and its original annual averages together with their correlations with provincial grand total and transportation NO<sub>x</sub> emissions, and the decreasing extents of the variables in ten Canadian cities during the last decades (& decreasing trends were always obtained with P<0.05; && Provincial total and transportation NO<sub>x</sub> emission decreasing percentage in presence of decreasing trends with P<0.05; # increasing trends in NO<sub>x</sub> emission from 1990-2010; ## since 1990; ^ P>0.05; An increasing trend was shadowed in red; R<sup>2</sup>>0.8 was highlighted in purple; bond numbers represent the overall decreasing percentage in NO<sub>2</sub> mixing ratios smaller than its corresponding provincial emission decreasing percentage).

| City                  | Correlation with original annual average (P<0.01) |               | Annual decreasing rate and overall decreasing percentage (unit: ppb year <sup>-1</sup> , %) <sup>&amp;</sup> |             |             | R <sup>2</sup> values between different types of mixing ratios with provincial total and transportation NO <sub>x</sub> emissions (P<0.05) |               |               | Emission decreasing percentage (total, transportation; unit: %) <sup>&amp;&amp;</sup> |
|-----------------------|---|---------------|--|-------------|-------------|--|---------------|---------------|---|
|                       | BRTs  | RF            | BRTs   | RF          | original    | BRTs   | RF            | original      |   |
| Halifax (1996-2017)   | y=1.03*<br>x                                      | y=1.08*<br>*x | 0.49,<br>62  | 0.45,<br>58 | 0.55,<br>50 | 0.83,<br>0.84  | 0.84,<br>0.85 | 0.86,<br>0.87 | 54, 56  |
| Montreal (1995-2019)  | y=0.99*<br>x                                      | y=1.04*<br>*x | 0.34,<br>44  | 0.32,<br>42 | 0.34,<br>39 | 0.90,<br>0.85  | 0.91,<br>0.86 | 0.87,<br>0.82 | 47, 52  |
| Quebec (1996-2019)    | y=0.98*<br>x                                      | y=1.02*<br>*x | 0.44,<br>51  | 0.39,<br>45 | 0.46,<br>46 | 0.97,<br>0.97  | 0.97,<br>0.98 | 0.95,<br>0.95 | 47, 52  |
| Toronto (2004-2019)   | y=1.02*<br>x                                      | y=1.04*<br>*x | 0.67,<br>40  | 0.64,<br>39 | 0.74,<br>37 | 0.96,<br>0.96  | 0.97,<br>0.98 | 0.94,<br>0.94 | 52, 52  |
| Hamilton (1996-2019)  | y=1.00*<br>x                                      | y=1.02*<br>*x | 0.53,<br>42  | 0.55,<br>44 | 0.54,<br>42 | 0.95,<br>0.97  | 0.95,<br>0.96 | 0.92,<br>0.93 | 58, 57  |
| Winnipeg (1984-2018)  | y=0.99*<br>x                                      | y=1.00*<br>*x | 0.37,<br>57  | 0.34,<br>57 | 0.34,<br>50 | 0.90,<br>0.93  | 0.91,<br>0.94 | 0.85,<br>0.89 | 43, 43 <sup>#</sup>   |
| Edmonton (1994-2019)  | y=1.02*<br>x                                      | y=1.00*<br>*x | 0.45,<br>41  | 0.47,<br>40 | 0.53,<br>45 | 0.57,<br>0.73  | 0.54,<br>0.73 | 0.63,<br>0.73 | 10, 29  |
| Calgary (1986-2007)   | y=1.00*<br>x                                      | y=1.01*<br>*x | 0.60,<br>31  | 0.60,<br>32 | 0.61,<br>33 | ^  | ^             | ^             | -11, -5 <sup>#</sup>  |
| Vancouver (1986-2019) | y=1.00*<br>x                                      | y=1.01*<br>*x | 0.36,<br>49  | 0.36,<br>47 | 0.37,<br>49 | 0.63,<br>0.75  | 0.63,<br>0.74 | 0.54,<br>0.66 | 23, 27 <sup>##</sup>  |
| Victoria (1993-2019)  | y=1.01*<br>x                                      | y=1.02*<br>*x | 0.31,<br>49  | 0.31,<br>45 | 0.31,<br>51 | 0.58,<br>0.69  | 0.58,<br>0.69 | 0.54,<br>0.65 | 23, 33 <sup>##</sup>  |



Table 2. Correlations between deweathered mass concentrations and original annual averages of PM<sub>2.5</sub>, and the changing extents of the variables in ten Canadian cities and provincial total grand PM<sub>2.5</sub> emissions during the last decades (<sup>#</sup> increasing trends were obtained with P<0.05 except “/” to be listed; <sup>&</sup> P>0.05; <sup>&&</sup> 0.24 and 2 represent annual decreasing rate of 0.25 µg m<sup>-3</sup> year<sup>-1</sup> and an overall decrease in 2 µg m<sup>-3</sup>, respectively; all increasing trends are shading in red).

| City                  | Correlation with original annual average (P<0.01) |          | Annual decreasing rate and overall decrease (unit: µg m <sup>-3</sup> year <sup>-1</sup> , µg m <sup>-3</sup> ) <sup>#</sup> |                    |                    | Decreasing percentage of total grand PM <sub>2.5</sub> emissions |
|-----------------------|---|----------|--|--------------------|--------------------|--|
|                       | BRTs  | RF       | BRTs   | RF                 | original           |  |
| Halifax (2008-2018)   | y=1.00*x  | y=1.02*x | / <sup>&amp;</sup>   | / <sup>&amp;</sup> | / <sup>&amp;</sup> | 27   |
| Montreal (2005-2019)  | y=1.00*x  | y=1.01*x | 0.24, 2 <sup>&amp;&amp;</sup>  | 0.22, 2            | 0.25, 2            | / <sup>&amp;</sup>   |
| Quebec (1998-2019)    | y=1.00*x  | y=1.01*x | / <sup>&amp;</sup>   | / <sup>&amp;</sup> | / <sup>&amp;</sup> | / <sup>&amp;</sup>   |
| Toronto (2000-2019)   | y=1.00*x  | y=1.01*x | 0.11, 2  | 0.10, 2            | /                  | / <sup>&amp;</sup>   |
| Hamilton (1998-2019)  | y=1.00*x  | y=1.01*x | 0.15, 4  | 0.14, 3            | 0.15, 3            | / <sup>&amp;</sup>   |
| Winnipeg (2001-2018)  | y=1.04*x  | y=1.04*x | -0.10, -2  | -0.10, -2          | -0.09, -1          | -11  |
| Edmonton (1998-2019)  | y=1.01*x  | y=1.03*x | / <sup>&amp;</sup>   | / <sup>&amp;</sup> | / <sup>&amp;</sup> | -40  |
| Calgary (1998-2014)   | y=1.00*x  | y=1.03*x | / <sup>&amp;</sup>   | / <sup>&amp;</sup> | / <sup>&amp;</sup> | -38  |
| Vancouver (2004-2019) | y=0.99*x  | y=1.02*x | / <sup>&amp;</sup>   | -0.08, -1          | / <sup>&amp;</sup> | 28   |
| Victoria (1999-2019)  | y=1.00*x  | y=1.03*x | / <sup>&amp;</sup>   | -0.08, -1          | -0.07, -1          | 42   |



Table 3. Trends in deweathered and original average of O<sub>3</sub> (NO<sub>2</sub>+O<sub>3</sub>) for each year at two levels in ten Canadian cities during the last decades (\*: O<sub>3</sub> (NO<sub>2</sub>+O<sub>3</sub>) mixing ratios ≥ 40 ppb; \*\*: O<sub>3</sub> (NO<sub>2</sub>+O<sub>3</sub>) mixing ratios <40 ppb; #: decreasing trend shading in green with P<0.05 and; ##: no trend or stable trend with P>0.10; ###: increasing trend shading in yellow with P<0.05).

| City                  | O <sub>3</sub> |    |          |            |    |          | NO <sub>2</sub> +O <sub>3</sub> |    |          |            |    |          |
|-----------------------|----------------|----|----------|------------|----|----------|---------------------------------|----|----------|------------|----|----------|
|                       | ≥ 40 ppb*      |    |          | < 40 ppb** |    |          | ≥ 40 ppb*                       |    |          | < 40 ppb** |    |          |
|                       | BRTs           | RF | Original | BRTs       | RF | Original | BRTs                            | RF | Original | BRTs       | RF | Original |
| Halifax (2000-2017)   | ↓#             | ↓  | ↓        | /##        | /  | /        | ↓                               | ↓  | ↓        | ↓          | ↓  | ↓        |
| Montreal (1997-2010)  | ↓              | ↓  | ↓        | ↑###       | ↑  | ↑        | ↓                               | ↓  | ↓        | /          | /  | /        |
| Quebec (1995-2019)    | ↓              | ↓  | ↓        | ↑          | ↑  | ↑        | ↓                               | ↓  | ↓        | /          | ↓  | /        |
| Toronto (2003-2019)   | ↓              | ↓  | ↓        | ↑          | ↑  | ↑        | ↓                               | ↓  | ↓        | ↓          | ↓  | ↓        |
| Hamilton (1996-2019)  | ↓              | ↓  | ↓        | ↑          | ↑  | ↑        | ↓                               | ↓  | ↓        | /          | /  | /        |
| Winnipeg (1985-2018)  | ↓              | /  | ↓        | ↑          | ↑  | ↑        | ↓                               | ↓  | ↓        | ↓          | ↓  | /        |
| Edmonton (1981-2019)  | /              | /  | /        | ↑          | ↑  | ↑        | ↓                               | ↓  | ↓        | ↓          | ↓  | ↓        |
| Calgary (1986-2014)   | /              | /  | ↓        | ↑          | ↑  | ↑        | ↓                               | ↓  | ↓        | ↓          | ↓  | ↓        |
| Vancouver (1986-2019) | ↓              | ↓  | ↓        | ↑          | ↑  | ↑        | ↓                               | ↓  | ↓        | ↓          | ↓  | ↓        |
| Victoria (1999-2019)  | ↓              | ↓  | ↓        | ↑          | ↑  | ↑        | ↓                               | ↓  | ↓        | /          | /  | /        |



Fig. 1. Performance evaluation of BRTs and RF algorithm using NO<sub>2</sub> mixing ratios measured in Halifax during 1996-2017. Red lines represent linear regression, and color bar reflects data number density.

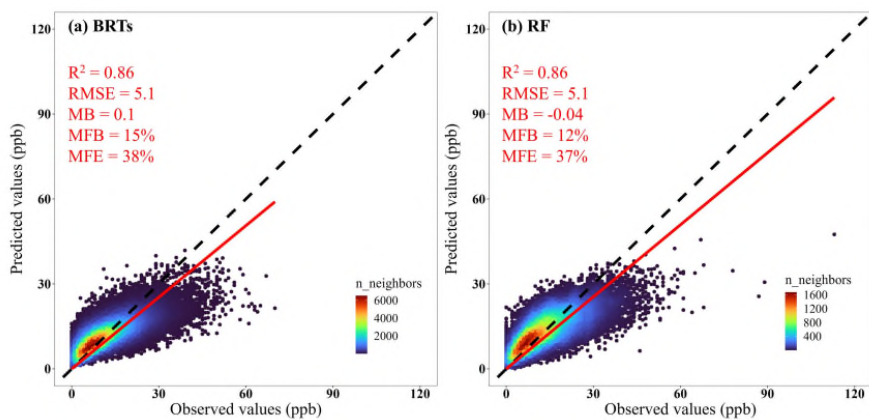




Fig. 2. Correlations between hourly  $PM_{2.5}$  concentration in a single year and its 22-year average in each hour in Edmonton. Left column shows percentile series of  $PM_{2.5}$  in 1998, 1999 and 2019, respectively, against the corresponding 22-year average series. Right column shows time series of  $PM_{2.5}$  in 1998, 1999 and 2019, respectively, against the corresponding 22-year average series. Red straight and blue dashed lines in a, c and e represent the regression curves within linear ranges and their extensions out of the linear ranges, respectively, and vertical arrows represent the distance of the predicted values from the regression curve. Red straight and black dashed lines in b, d and f represent the regression curves and 1:1 lines, respectively.

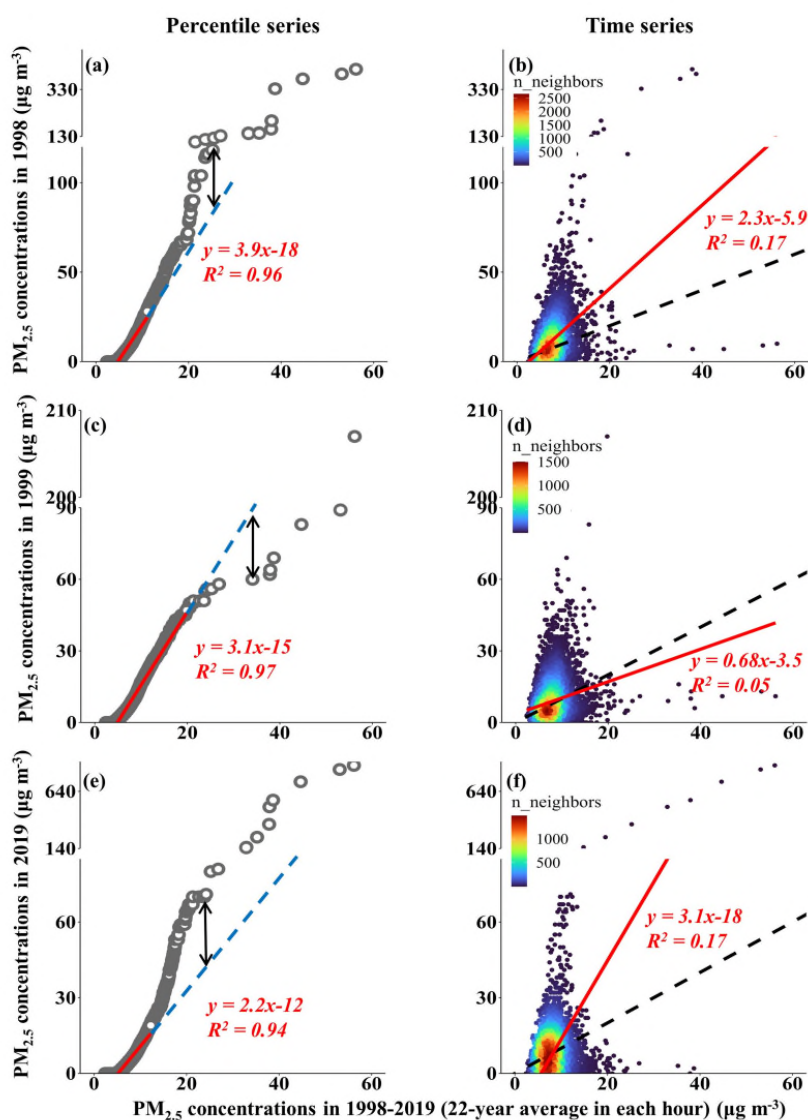




Fig. 3. Trends of original annual average  $\text{NO}_2$  and  $\text{PM}_{2.5}$  in five eastern (upper row) and five western (lower row) Canadian Cities.

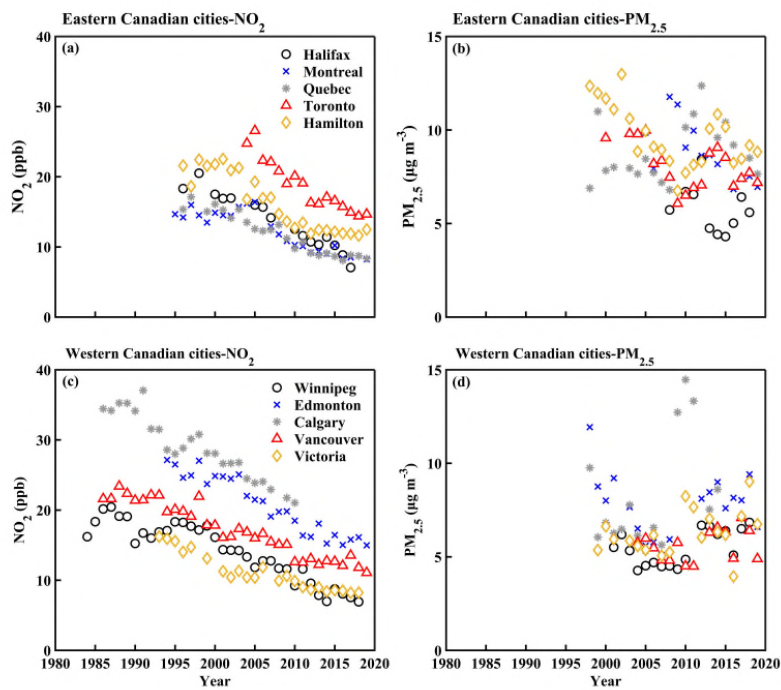




Fig. 4 Deweathered hourly mixing ratios of  $O_3$  (left column) and  $NO_2+O_3$  (right column) at levels  $\geq 40$  ppb in five eastern Canadian cities.

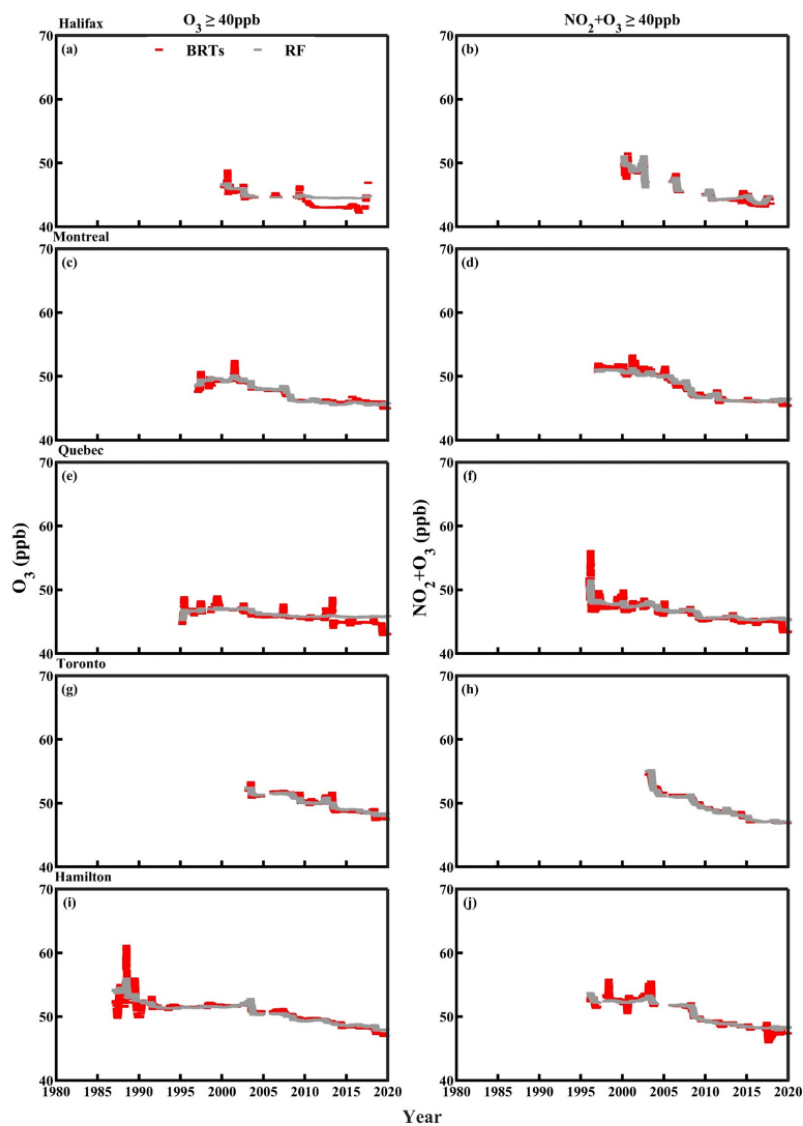






Fig. 5. The calculated perturbation contribution to the corresponding original annual average (left column) and the mean and standard deviation of the calculated perturbation (right column) in five western Canadian cities.

